Review Paper

Synthesis techniques, characterization and mechanical properties of natural derived hydroxyapatite scaffolds for bone implants: a review

Obinna Anayo Osuchukwu[1] · Abdu Salihi[1] · Ibrahim Abdullahi[1] · Bello Abdulkareem[1] · Chinedu Sixtus Nwannenna[2]

Received: 29 June 2021 / Accepted: 7 September 2021
Published online: 29 September 2021

Abstract
Hydroxyapatite (HAp) with good mechanical properties is a promising material meant for a number of useful bids in dentistry and orthopedic for biomedical engineering applications for drug delivery, bone defect fillers, bone cements, etc. In this paper, a comprehensive review has been done, by reviewing different literatures related to synthesis techniques, mechanical properties and property testing, method of calcination and characterization of hydroxyapatite which are product of catfish and bovine bones. The discussion is in relations of the obligatory features vital to attain the best properties for the envisioned bid of bone graft. The process approaches that are capable of fabricating the essential microstructure and the ways to advance the mechanical properties of natural mined HAp are reviewed. The standard values for tensile strength were found to be within the range of 40–300 MPa, compressive strength was 400–900 MPa, while Elastic modulus was 80–120 GPa and fracture toughness was 0.6–1 MPa $m^{1/2}$ (Ramesh et al. in Ceram Int 44(9):10525–10530, 2018; Landi et al. in J Eur Ceram Soc 20(14–15):2377–2387, 2000; Munar et al. in Dent Mater J 25(1):51–58, 2006). Also, the porosity range was 70–85% (Yang et al. in Am Ceram Soc Bull 89(2):24–32, 2010), density is 3.16 g/cm^3 and relative density is 95–99.5% (Ramesh et al. 2018; Landi et al. 2000; Munar et al. 2006). The literature revealed that CaP ratio varies in relation to the source and sintering temperature. For example, for bovine bone, a CaP ratio of 1.7 (Mezahi et al. in J Therm Anal Calorim 95(1):21–29, 2009) and 1.65 (Barakat et al. in J Mater Process Technol 209(7):3408–3415, 2009) was obtained at 1100 °C and 750 °C respectively. Basic understanding on the effect of adding foreign material as a strengthening agent to the mechanical properties of HAp is ground factor for the development of new biomaterial (Natural hydroxyapatite, NHAp). Therefore, it is inferred that upon careful combination of main parameters such as compaction pressures, sintering temperatures, and sintering dwell times for production natural HAp (NHAp), mechanical properties can be enhanced.

✉ Obinna Anayo Osuchukwu, obinasanayo@gmail.com | [1]Department of Mechanical Engineering, Bayero University, Kano, Nigeria. [2]Ahmadu Bello University, Zaria, Kaduna, Nigeria.

Graphic abstract

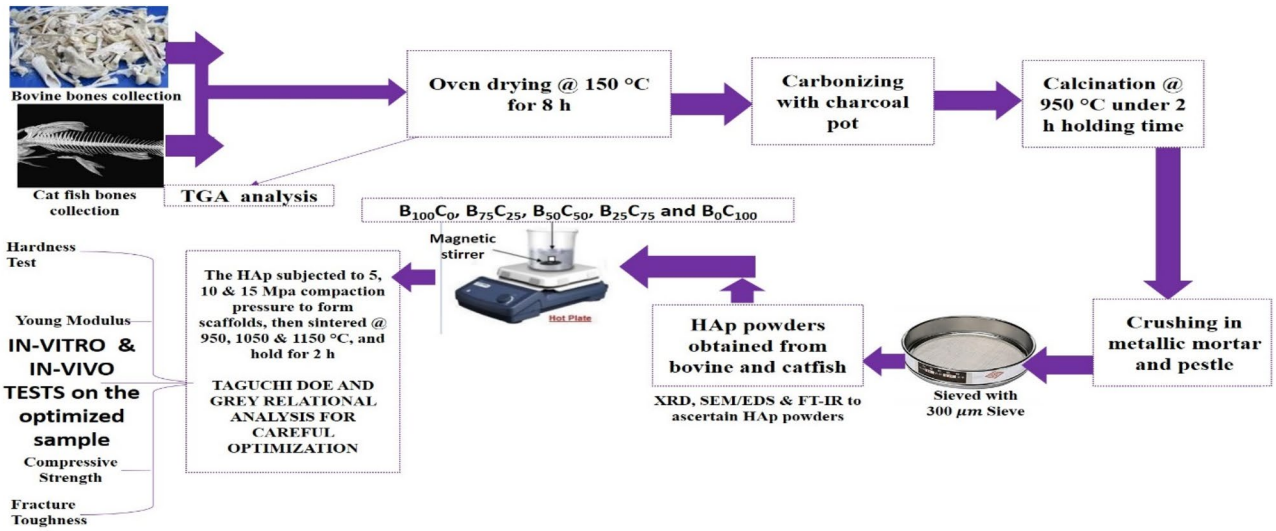

Keywords Hydroxyapatite · Biomedical engineering · Mechanical properties · Synthesis techniques · Biomaterials

1 Introduction

Concerning human body infirmity of restoring bone faults, the use of non-natural bone tissue has gotten much consideration in recent times. Novel group of bio-scaffolds are the suitable method for faulty bone tissue. Bone fracture at times emerge from accident, genetic or disease [1]. Numerous researches have been steered to produce porous biomaterials scaffold using different approaches for clinical use [2–4]. Biomaterials used in this category of application should be bioactive and made of synthetic or natural polymers, ceramics, and metals with sufficient porosity to ensure blood circulation inside human body using software and anatomical model [5–10]. Ceramic materials including hydroxyapatite (HAp) and others like biphasic calcium phosphate (CaP), bio-glasses (BG), and β tricalcium phosphate (βTCP) have been used in bone tissue engineering for implant [11–14]. Bioceramics are of great importance in tissue engineering. Bioceramics are ceramics materials used in tissue engineering for restoration, repair and replacement of bones [15]. Tissue engineering pushes for a material with elementary features of biocompatibility, biodegradability and ideal morphology that can serve for bone substitutes in the field of bone implants [16]. It have been proved in tissue engineering that hydroxyapatite (HAp) is the best sure system of calcium phosphate. This attest to its affinity for bone tissue and similarity to natural bone minerals, therefore, it is considered to be the most commonly used in bone restoration [17]. Compared with other materials like polymers and metals, HAp has the advantage of being easy to adjust its crystallinity and microstructure to suit specific applications in bone implant because of its biodegradable property. Moreover, HAp is biocompatible, that is, non-toxic, non-inflammatory and enhanced immune response [18–22]. In latest studies, HAp has been mined from both natural and synthetic sources through diverse handling [23–30]. However, HAp derived by synthetic methods have some disadvantages of poor mechanical and chemical properties. Due to the need for ultra-high purity, chemical substances after synthesis lack some important traces of Sodium (Na), Silicon (Si), Iron (Fe) or Minerals), and some of which are expensive raw materials such as carbonates which are present in natural HAp. These elements are important in bone growth and biological functions [20, 23].

Natural sources used by different researchers to produce HAp include: bovine bone [24, 31, 32], fish bones [33, 34], pig bones [24, 35], egg shells [28, 36], sea shells [37, 38] and biological waste (non-separated animal bones) [21, 22]. The common acceptable method to synthesize HAp is the sintering method [25]. Stea et al. [39] reported that the HAp derived through sintering method formed a very tight bond with bone tissue. The HAp sintering methods can be subdivided as follows: sintering in traditional muffle furnace, microwave and spark plasma methods [19, 23, 27, 40]. Beaufils et al. [41] recently employed an electrodeposition technique, assisted by template to produce HAp with a nano size morphology and high aspect ratio of Ca/P as well as better mechanical and biological properties. Foroutan et al. [42] used the graphene nanosheet to

improve the new group of calcium silicate (CS) scaffold. Thus, the use of HAp in the repair and reconstruction of bones has been able to open up thrilling prospects for the orthopedic and dentistry over other methods. Therefore, the study on microstructural developments is imperative in developing materials with superior mechanical properties that is acceptable [43]. Gross et al. [44] applied Instrumented nanoindentation to determine the mechanical properties of plasma sprayed hydroxyapatite-coated implants from different commercial vendors. Abifarin et al. and Akpan et al. [21, 45] in different studies agreed that HAp from Fish and Bovine bones have excellent characteristics of biocompatibility and biodegradability because of their physicochemical behaviours similar to that of normal human bone HAp.

Akpan et al. [46] optimized and evaluated HAp synthesised from from catfish bones to achieve optimum handling situations and workable instructive methods for the research of hydroxyapatite scaffolds for tissue engineering. Studies to improve the properties of HAp derived from natural sources have been widely researched in the past years by numerous researchers, essentially due to the fact that these materials are readily available, thereby reducing the cost of producing HAp which is very important in tissue engineering. Enough methods have been used to advance biomaterial mechanical properties such as compressive strength, fracture toughness, porosity and tensile strength [47–52].

For improved mechanical properties, from the open literature reviewed, no investigation has been made regarding the physical, mechanical and chemical properties of animal matrix of non-separated biowastes and catfish bones derived hydroxyapatite (% wt, as shown in the graphical abstract). The availability of these bones as the natural means of HAp makes the study interesting. Hence, this study aims to accomplish a review to improve the mechanical properties of HAp (made from Cow and fish bones, by mixing them in a proportion, see the graphical abstract)—processing, mechanical properties evaluation and characterization in order to produce a scaffold

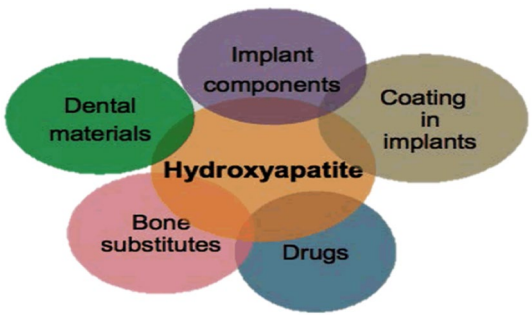

Fig. 1 Applications of HAp [53]

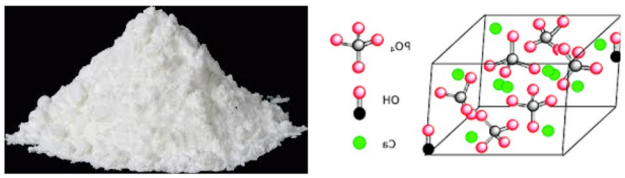

Fig. 2 Hydroxyapatite **a** Powder from cow bone, **b** Lattice [21, 62]

that will be use for the following biomedical applications, i.e. as bone defect fillers and tissue engineering scaffolds, implants coating, pins for anchoring tooth implant and drug delivery systems (Fig. 1).

2 Formation of hydroxyapatite

Hydroxyapatite (Fig. 2a) is a calcium phosphate mineral found in the human bone. The lattice-like (Fig. 2b) organization of hydroxyapatite crystals accounts for the firmness of bones. Hydroxyapatite is commonly used in the fabrication of bone void plaster products that affords scaffolding for bone development to complement a parent or host bone in orthopedic techniques [54–56]. Hydroxyapatite which has chemical configuration of $(Ca_{10}(PO_4)_6(OH)_2)$, is harmless, biocompatible, osteoconductive, non-immunogenic and gives undeviating ties with active materials. It also have Ca/P ratio of 1.66. Hydroxyapatite (HAp) can be produced from natural and synthetic sources [20, 21, 57, 58]. Hence, both natural and synthesized types of HAp are largely used as bio-ceramic in form of particulates, coatings etc. for hard tissue repair. It has been extensively reported that HAp has like chemical constituents with the inorganic part in animal tissues and this has resulted in its preferred biocompatibility attributes such as harmlessness, no inflammatory effects etc. [19, 20, 59]. Sobczak et al. [60, 61] reported that the procedure to produce HAp powders from wastes is interesting because of its economic value and environmental benefits and that the HAp is not easily overruled by human tissues due its natural likeness to human bone. Sahmani et al. [44], added titanium oxide (TiO2) nanoparticles to nanoclay (NC) composed with NaCl microparticles to build a porous scaffold using space holder procedure. Their result proposed that the scaffold ought to have an organized permeable structure besides its porosity size (> 80%) for improved cell seeding and the development of tissue.

Scaffold forms the base for bone growth and helps cell bond, development and variation in orthopedic operations. Producing scaffold with satisfactory porous geometry and right compressive strength is contentious amongst biomaterial engineers and medical orthopedic surgeons [63]. Aghdam et al. fabricated a porous cylindrical scaffold

(6 mm × 10 mm) with space holder (SH) method applying sodium bicarbonate ($NaHCO_3$) as a porous agent. The porous hydroxyapatite-was reinforced with 0, 5, 10, and 15 wt% alumina nanoparticles (ALN: 40–80 nm) for bone substitute [63]. Gross and Saber-Samandari revealed mechanical properties of a suspension plasma sprayed coating with nanoindentation. Hydroxyapatite was placed in an r.f. plasma using a powder and a suspension. The powder feedstock formed a dense, oriented coating, while the suspension led to a porous haphazardly oriented coating. The porosity caused a decline in the hardness and elastic modulus of the bulk coating, while the plasma coating gave higher Figures (5 ± 0.2 vs. 4 ± 0.2 GPa) [64].

Saber-Samandari & Gross investigated the fitness of nanoindentation to encompass the study of the cross-section to manifold points for a more comprehensive understanding into disparities through the thickness of the coating. Multiple indentations with a separation of 4 µm exhibited a transition within the thickness of the coating. Nanoindentation testing revealed a non-uniform stress state throughout the HAp coating. Micro-Raman Spectroscopy (MRS) (Fig. 3) revealed dehydroxylation of the powder during the traverse in the thermal zone. [65].

In another study by Saber-Samandari & Gross, nanoindentation was adopted to determine the hardness and elastic modulus on the surface of well spread solidified droplets at the hydroxyapatite coating surface. The Micro RMS (Fig. 4) and X-ray diffraction (Fig. 5) confirmed a larger degree of dehydroxylation for the smaller particles also showing a lower elastic modulus This shows the influence of particle size and possibly dehydroxylation of hydroxyapatite on the mechanical properties of the coating surface [66].

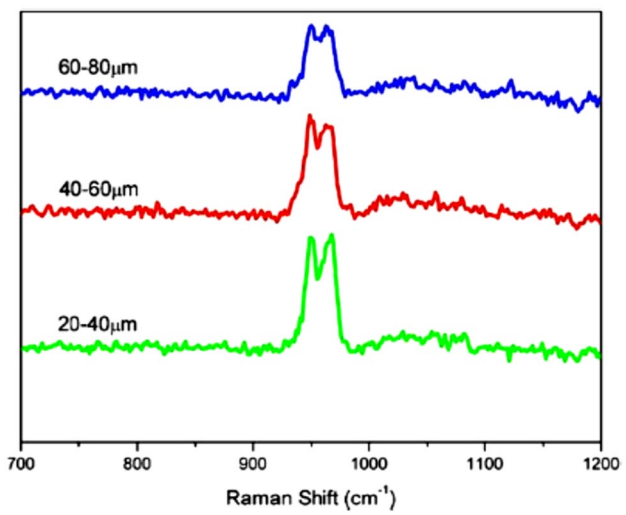

Fig. 3 Micro-Raman spectra of coatings [65]

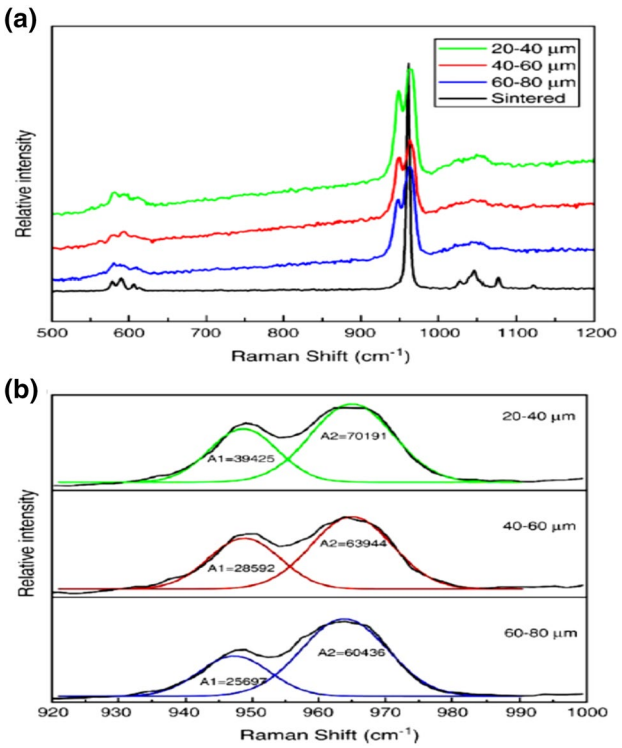

Fig. 4 Raman microprobe spectra (RMS) of **a** sintered HAp and thermally sprayed HAp **b** Peak area analysis [66]

Natural hydroxyapatite can be basically synthesized from organic matters, namely; mammalian bones (such as cattle, camels and horses), aquatic or marine sources (such as fish bones and scales), shell sources (such as clams, egg shell), plants and algae, and minerals (such as limestone) [21, 22, 24, 28, 31–38]. Some of the approaches that can

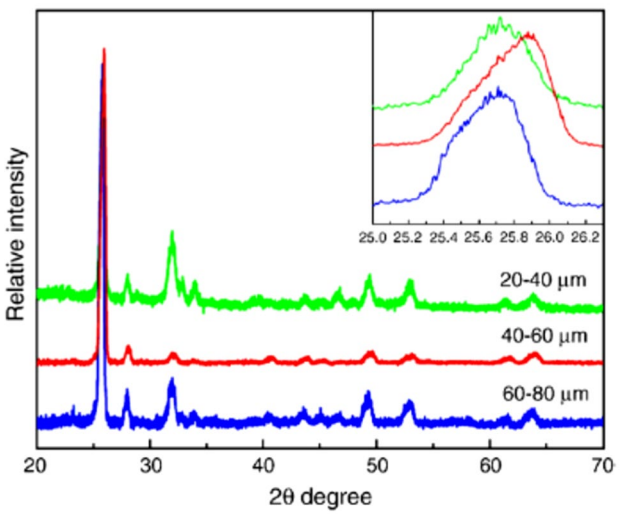

Fig. 5 X-ray diffraction patterns of hydroxyapatite HAp coatings [65]

Table 1 The sources and some techniques used for synthesizing natural HAp [69]

Natural hydroxyapatite ($Ca_{10}(PO_4)_6(0H)_2$					
Items	Mammalian	Aquatic sources	Shells	Plant and algae	Mineral
Examples:	Bone (cow, pig, camel, horse, sheep, goat, etc.)	Fish bone, fish scale, crocodile bone, etc	Snail shell, egg shell, cockle shell, clam shell, sea shell, mussel shell, etc	Fruit peels (banana, orange, etc.), Plant (leaves, stalk, flowers), algae, woods	Limestone
Techniques:	Calcination, Hydrothermal, Alkaline hydrolysis, Combination of techniques	Calcination, Hydrothermal, Alkaline hydrolysis, Combination of techniques	Calcination, Hydrothermal, Mechano-chemical, Sol–gel precipitation, Combination of techniques	Calcination Microwave irradiation, Pyrolysis, Chemical precipitation, Alkaline hydrolysis, Combination of techniques	Calcination, precipitation, hydrothermal, and ultrasonic irradiation

Table 2 Diverse ways to produce HAp powder [15]

Techniques	Characteristics	Merits	Demerits
Wet methods Precipitation/Calcination	High crystallinity after sintering at 900 °C Particle mass enlarged with growing sintering temperature Particle bulk of 7.7–59.0 nm	Cheap Few number of Chemicals Nano size of HAp	Dissimilar of HAp Morphology -Small crystallinity of HAp Great crystallinity of HAp when sintering at elevated temperature
Hydrolysis	The particle bulk reduced after synthesized with cetyltrimethylammonium Particle dimension of 20–50 nm Ca/P proportion: 1.33–1.67	Small temperature method Limited amount of Chemicals Great phase purity of HAp Nano dimension of HAp	High cost Diverse of HAp Morphology
Emulsion	The crystallinity enlarged with growing heat treatment temperature The stability of the apatite phase achieved when being heat treated at 800–1300 °C Particle dimension of 200–1300 µm Ca/P proportion: 1.5–1.2	Great phase purity of HAp	Expensive Many number of Chemicals Non-stoichiometric HAp Low crystallinity of HAp
Hydrothermal	Rod -like morphology with hexagonal form Ca/P proportion: 1.67	High crystallinity of HAp Stoichiometric HAp	Expensive
Sol–gel	Disparity of Ca/P molar proportion rest on the calcinations temperature Crystalline dimension of 20–60 nm Ca/P proportion: 1.66–1.77	Nano dimension of HAp Great segment purity of HAp	Various of HAp morphology
Dry methods solid state	The calcining temperatures were important in directing the dimension and nature of HAp unit Grain magnitude of 747–1510 nm Ca/P proportion: 1.67	Cheap Less amount of Chemicals Micron dimension of HAp	Small phase purity of HAp Great crystallinity of HAp when sintering at elevated temperature

be used to prepare hydroxyapatite powder include sol–gel process [67], chemical precipitation [68], hydrothermal reaction and solid-state reaction [60]. Table 1 below shows examples and techniques used to synthesize natural HAp [69]. Applying these methods, as shown in Table 2, HAp powder obtained has different morphologies, stoichiometric, grain sizes and crystallinity levels [60]. Chaudhari et al. applied the equation below to prepare HAp [70].

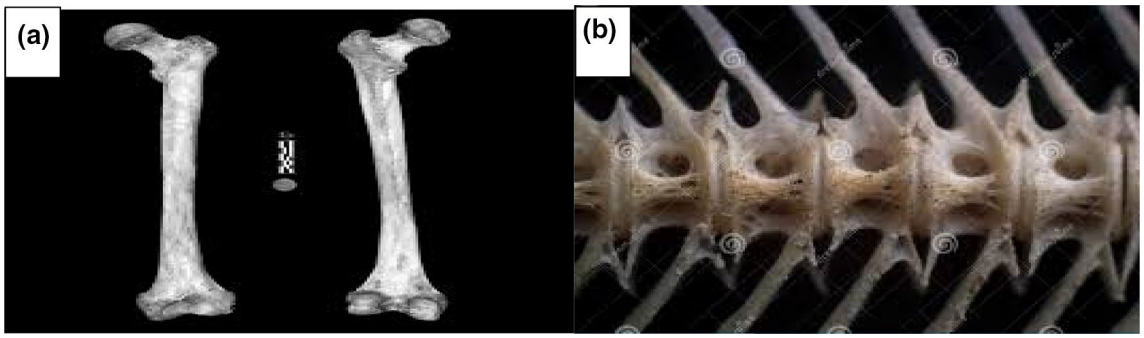

Fig. 6 **a** The cortical part of bovine bone **b** A typical catfish bone [45]

$$10CaO + K_2HPO + 4H_2O \rightarrow Ca_{10}(PO_4)_6(OH)_2 + 12KOH$$

2.1 Preparation of hydroxyapatite from cow bone

The extraction of HAp from bovine bone have been stated by many researchers. The bone part shown in Fig. 6a is usually used because its likeness to human bone in HAp composition [45].

Ravaglioli and Krajewski reported that the extraction methods affects the Ca/P proportion, dimension, natures and crystalline segments of Ca-P of the extracted HAp [57, 71]. Some researchers agreed that washing and removal of dirt, fats, protein, and additional constituents like marrows and spineless tissues should be done before extraction. The pretreatment involves boiling the bones in water for up to 8 h or more to eliminate organic constituents on the bone [21, 22, 72, 73].

Other initial treatment method that are extensively adopted is cleaning the osteo with surfactant and alkali solutions to confiscate the soft tissues [74]. To have pure synthesized HAp, Absorption Spectrometry (AAS) is normally employed to investigate the concentration of heavy metals in the tap water specimen [21]. According to Abifarin et al. [21], the concentration in portions per million (ppm) of hefty metals like Copper (Cu), Iron (Fe) and Zinc (Zn) were in minor aggregates and is in agreement as claimed that concentrations of weighty metal ions trace in running water are commonly negligible [59, 75].

Some methods like thermal decomposition, calcination or its combination with one or other methods have been employed to extract HAp from bovine bone [21, 76]. In the calcination process, to remove some organic materials such as proteins, oils, fat, pathogen, etc., the bones are heated in the furnace at an elevated temperature of up to 1400 °C [76]. Abifarin et al. synthesized HAp from non-separated animal bone. In his experiment, he cleaned the bones (Fig. 6a) with running water before boiling the samples for 3 h to deproteinize them. After boiling, there was another washing before drying at 150 °C for 8 h. Thereafter, it was made to powders and calcined underneath atmospheric state with an electric furnace at 900 °C at a ramp rate of 5 °C/min with 2 h of water-logged time and permitted to furnace cool. The samples at 900 °C presented high crystallinity of 86.15% deprived of impurities. The XRD (Fig. 7) reflections characteristics showed a hexagonal phase HAp. According to their result, at sintering temperatures range of 900–1100 °C for 2 h, the crystallinity of the HAp segments in the samples became extra apparent with growing shrill and thin reflections indicating the consequence of sintering proceeding the change of RB to pure HAp without the presence of decomposed products and the Ca/P proportion of 1.58 was obtained. The FT-IR information showed phosphate and hydroxyl peaks in the thermally treated samples and all the samples formed distinctive extending manners of O–H bands at about 3417 cm^{-1} which were noticed in all FT-IR spectra of HAp [21].

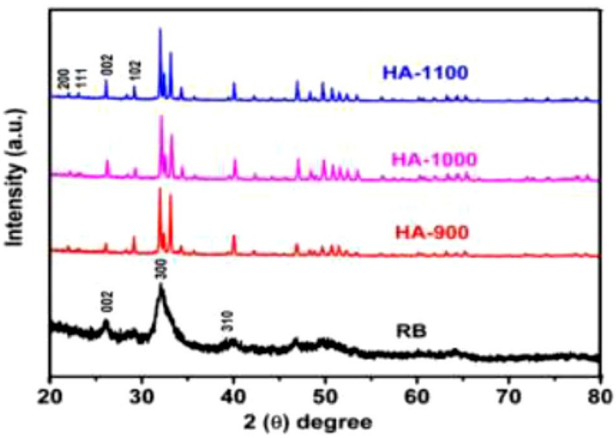

Fig. 7 The XRD pattern HAp at different sintering temperatures [21]

The process of combining alkaline heat treatment and calcination was employed towards mining HAp from pig bones. The pig bones were immersed in 4 M of sodium hydroxide (NaOH) at 100 °C for 24 h. The practice was

redefined again with a fresh NaOH solution and washed until the deposit attained a pH value of 7 and then dried. The samples were calcined at 800 °C and 1200 °C. But at 800 °C, a pure HAp phase was produced, while at 1200 °C, there was a mixture of HAp and CaO [77, 78]. At calcination temperature of above 700 °C, there were traces of CaO [12]. The above method was used to extract 70–180 nm nanometer HAp from pig bones, but the shape of the particles was different (irregularly and plate-shaped HAp) [77, 78]. The Ca/P ratios of both samples were 1.709 [78] and 1.72 [77], and the Ca/P ratio is above the stoichiometric ratio. Another method employed to extract HAp from bovine bones was combination of calcination and vibration grinding [72]. The calcination temperature was 800 °C for 3 h before the numerous grinding periods. Two grinding periods used were: ball milling (24 h) and vibration milling for altered intervals [72]. This combination of methods gave a needle-shaped HAp (Fig. 8) with a diameter of less than 100 nm and a Ca/P ratio of 1.66 [72]. The calcination method can convert HAp into new calcium phosphate phases, such as β-TCP, at elevated temperatures. Though, alkaline heat treatment systems, ionic liquid pretreatment and enzymatic hydrolysis systems produce pure phase HAp with minor crystallinity likened to the calcination system. Generally, record of the ways used in this review study can yield nano-scale HAp with altered morphologies.

2.2 Preparation of hydroxyapatite from catfish bone

The increase in fish consumption all over the globe has caused major surge in fish remains creation in the nature of bones (Fig. 6b). The retrieval of fish scales and bones permits the production of HAp and decrease in fish remains in the fishery production [79]. The fish bone is filled with calcium, phosphate, and carbonate which makes it important for the mining of HAp [76]. Fish bone apatite is produced after processing the fish wastes through a series of steps (Table 2) [21, 22, 45]. The fish bones can be either mechanically-, enzymatically-, or thermally-treated before using

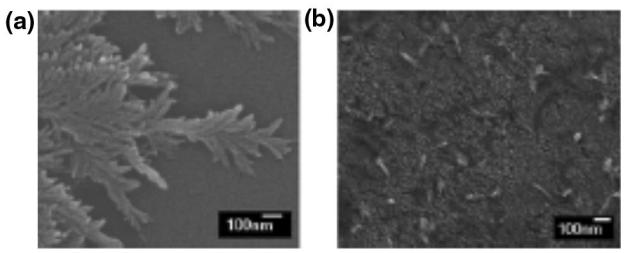

Fig. 8 SEM of HA powders at different vibro-millng hours, **a** 2 h **b** 8 h [72]

them as an absorbent in the batch and column experiments [80]. With good technique, the mechanically and enzymatically treated fish bone apatite yielded greater dissolved organic carbon (DOC) and biochemical oxygen needs (BON) with concentrations than those produced by thermal treatments [80]. In the above study, mechanical treatment was done by eliminating the skin and organic measures of the fish by slicing, pressing, searing and hot-air drying. Enzymatic treatment was done using an enzymatic digestion route that detached all bio organics [80]. Thermal treatment was done by assigning roughly 1 kg of untouched mechanically treated apatite in a muffle furnace for 24 h and heating it at a high temperature [80].

Just as in the preparation of HAp from bovine bone, pretreatment is also done before the production of HAp from fish bone. Soaking the bone in a small concentration of hydrochloric acid (0.1–1 M HCl) to deproteinize it and then wash in tap water and boiling has been used by different researchers to remove flesh and debris from the fish bone [34, 79, 81–84]. Natural apatite from fish bone can be used as a supplementary for HAp for remediating aqueous heavy metals [85]. It was found that fish bone apatite has the capacity of removing various metals and radionuclides including Pb^{2+}, Cu^{2+}, Cd^{2+} and Ni^{2+} to below visible levels. Chromium removal by fish bone apatite from groundwater has been studied by Ozawa and Suzuki [62]. Lead, Pb removal by fish apatite has been investigated by Ozawa and Kanahara [86]. Wright et al. established that by using fish bone apatites, the remediation cost was $40 per 3,785,411.78 L of water per mg/L of metal, and for soils it was $20-$30/yd^3. Thus, fish bone can serve as a cost-effective substitute for HAP for use in PRBs employed for treating metal plumes [87].

The combined alkaline heat treatment and calcination used to obtain HAp showed that the HAp has pure crystallinity having 76.62 nm particle size and 1.62 Ca/P stoichiometric ratio. In this technique, fish scales were first of all soaked in 1 M of NaOH. Thereafter, calcium chloride dehydrate ($CaCl_2{\cdot}2H_2O$) was employed to treat it at 75 °C for the compensation of calcium absent in the fish scales. The treated fish scale is then heated at 800 °C under 1 h [79]. The calcination of HAp at 600–1000 °C produces pure HAp with high crystallinity. 1.63 Ca/P stoichiometric ratio was observed in the sample heated at 600 °C, and is a little bit below the HAp Ca/P stoichiometric ratio. Furthermore, from the elemental analysis, the sample heated at 600 °C showed that there are Magnesium, Mg ions in the sample, and these Mg ions act as micronutrients for tissue metabolism [81]. A thermally treated fish scales at 1000 °C, which was pulverized for 16 h with a pulverizer to obtain pure phase HAp with 1.71 Ca/P stoichiometric ratio. The morphology of the HAp structure shows an almost spherical shape having 76.62 nm particle size [88].

The crystals size of hydroxyapatite can be preserved when alkali heat treatment technique is employed, which tend to coalesce during heating. Hydroxyapatite with Ca/P proportion of 1.65 that is handy to the stoichiometric HAp has been produced by calcination, but a higher Ca/P stoichiometric ratio is observed for HAp derived through alkaline heat treatment [62]. The calcination and alkaline hydrolysis systems was used to mine HAp from fish bones at 900 °C for 5 h. Alkaline heat treatment technique is when the fish bones are soaked in 2 M NaOH and then heated around 250 °C for about 5 h. The precipitate is then cleaned and accustomed with water to a neutral pH, and dried afterwards. Nevertheless, the crystallinity of HAp produced by calcination is upper linked with the one produced when alkaline heat treatment is employed. When comparing alkaline heat treatment method, the HAp obtained by calcination has a larger particle size [89]. Also, HAp was extracted using alkaline heat treatment from fish scales, although in two stages. The samples were first treated using 5% of NaOH to soak them in the solution for 5 h. The treated samples were sieved and dried; after which the treated dehydrated samples were immersed again in 50% of NaOH solution for 1 h. The chemically treated residue was sieved and rinsed with deionized water to achieve neutral pH value, and was dried afterwards. This technique produced a highly pure nano HAp with a Ca/P stoichiometric ratio of 1.66. The crystallinity of HAp made by alkaline heat treatment (Fig. 9) is smaller than that of HAp produced by calcination [84].

Ozawa and Suzuki [62] employed thermal decomposition system to formulate HAp from fish bone. First, the flesh on the fish was cleaned with the aid of a strong water jet after steaming in water for 1 h. The cleaned samples were later dehydrated and calcined at a temperature of 600–1300 °C in air. According to their result, at calcination temperature of 800–1200 °C, highly crystalline HAp was gotten and this HAp was seen cohabited with a tricalcium phosphate (TCP) gotten when the calcination temperature was 1300 °C.

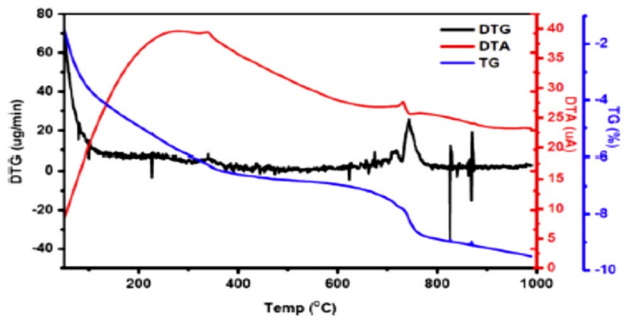

Fig. 9 Typical TG/DTA/DTG of HAp produced by alkaline heat treatment [84]

3 Characterization of bovine and catfish bone derived hydroxyapatites

Hydroxyapatite characterization is necessary to investigate the material structure and properties. Characterization can be chemical or physical. The characterization of HAp is exceptionally proficient and appropriate to analyse HAp to meet the set standard for a broad range of application in biomedical. Akpan et al. [45] adopted the procedure used by Abifarin et al. [21] to clean the bovine and fish bones. The cleaned samples were flame cooked in an open air and subjected to sintering temperature of 900 °C for 2 h at a heating rate of 5 °C/min. Afterward, the produced HAp powders were pound in a steel mortar and sieved with a filter of 300 µm mesh. The SEM (Fig. 10) result for the hydroxyapatite derived from Catfish bone (CB) showed a typical flower-like microstructure which comprises flakes of petal-like alignment, while rod-shaped particles are manifest for the bovine bone (BB) hydroxyapatite. They reported that the images showed the presence of extra naked pores in the CB and the micro pore amounts decline with apparent density. The CB showed higher porosity (Fig. 11) than the BB. In this research, the FT-IR (Fig. 12) spectra attained from the CB and NB powders displayed a

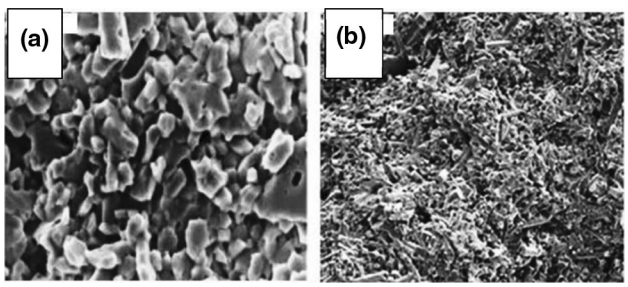

Fig. 10 SEM picture of **a** catfish bone **b** bovine bone hydroxyapatite obtained at 900 °C [45]

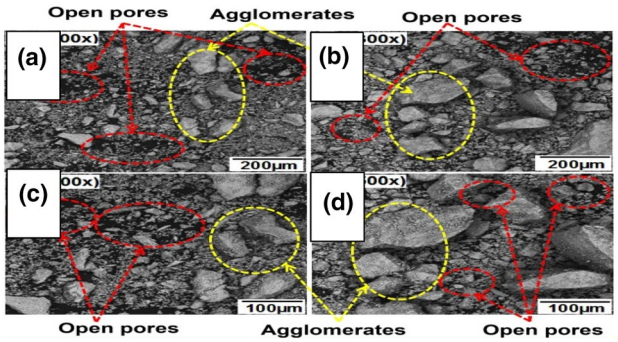

Fig. 11 Scanning electron micrographs HAp showing pores on **a** CB 200 µm **b** NB 00 µm **c** CB 100 µm and **d** 100 µm [45]

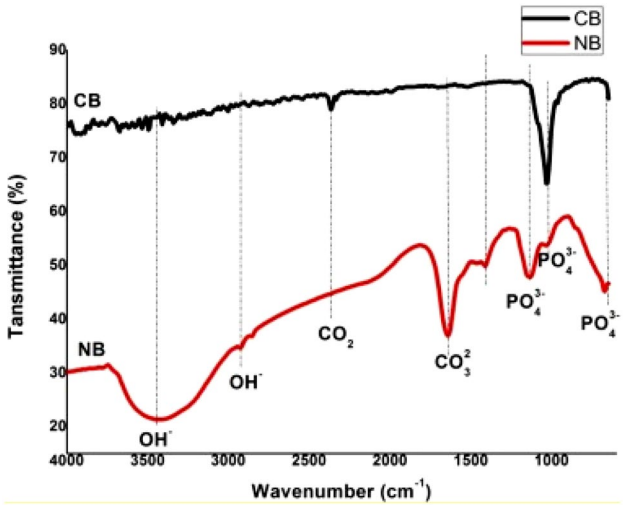

Fig. 12 FT-IR spectra for CB and NB derived hydroxyapatites [45]

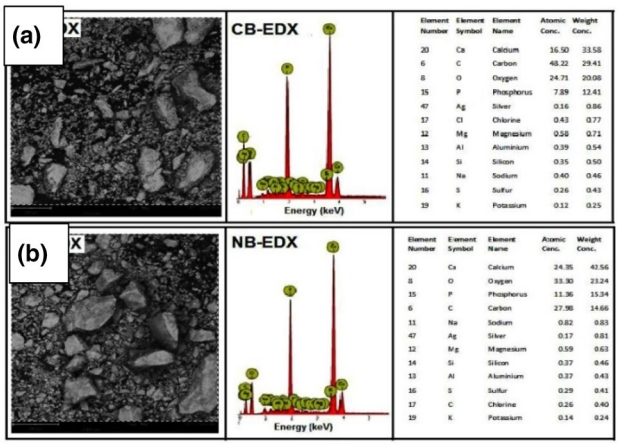

Fig. 13 SEM/EDX of HAp for **a** CB and **b** NB [45]

kind of bands from 1100 ± 1550 cm^{-1} in accumulation to the points normal for hydroxyapatite. For the NB, a broad peak was seen around 3417 cm^{-1} showing the existence of adsorbed water. SEM/EDX (Fig. 13) analysis discovered the fundamental structure and the conforming Ca/P molar ratio of 1.58 and 1.63 for CB and NB respectively and these has small nonconformities from the hypothetical rate for stoichiometric HAp of 1.67. They concluded that main cause of this deviation is due to burning in open air. The EDX also showed that HAp gotten from the CB and NB comprises ions such as Na^+, Mg^{2+} traces [45].

Hosseinzadeh et al.[90] used the thermal decomposition method to extract HAp from bovine bone, in which the sample was heated at two varried temperatures (750 °C and 850 °C) for 6 h, and two unit dimensions (ie good (< 420 µm), HAp are rough particles (420–500 µm) at 750 °C and 850 °C respectively were obtained. From the XRD results, bone meal heated to 750 °C indicated unadulterated HAp, while at 850 °C, the binding of β-tricalcium phosphate (β-TCP) and HAp were detected. Due to the presence of β-TCP, the Ca/P ratio of the powder heated to 850 °C decreased to 1.5. Ayatollahi et al. [73] again used heat treatment to mined HAp from bovine bones and calcined it at 900 °C for 2 h. The calcined bones were ground by means of a high-energy planetary ball mill to shrink the size to 30 nm. The XRD outcomes gave unadulterated HAp phase at 900 °C.

Londo ~ no-Restrepo et al. [91] employed both calcination and hydrothermal methods to mine HAp from bovine bones. Hydrothermal technique is used to remove some protein and fat from the bones. Thereafter, the powder is calcined at a temperature range of 700–1100 °C. The morphology of HAp changes with the calcination temperature (for example, lopsided at 700 °C and hemispherical at 800 °C). Dehydroxylation of HAp was formed at temperatures above 800 °C. Sun et al. [74] also used calcination technique to produce HAp from cow bones through thermal treatment at 750 °C for 2 h. This process led to the realization of irregular shaped HAp with 20–100 µm size range and a Ca/P ratio > 1.67. Because there were some ions, namely; carbonate was exchanged within the HAp. The Ca/P ratio is usually above 1.67. The XRD pattern indicated that there was formation of HAp and β-TCP when thermally treated. Abifarin et al. [21] proposed a data set, which introduced the morphological characteristics, basic structure and functional groups of hydroxyapatites (HAp) synthesized from non-separated biological waste (animal bone) through an improved and convenient heat treatment method. The temperature reaches 1100 °C. The elemental configuration obtained by the weight and atomic analysis of all samples by EDX provided information

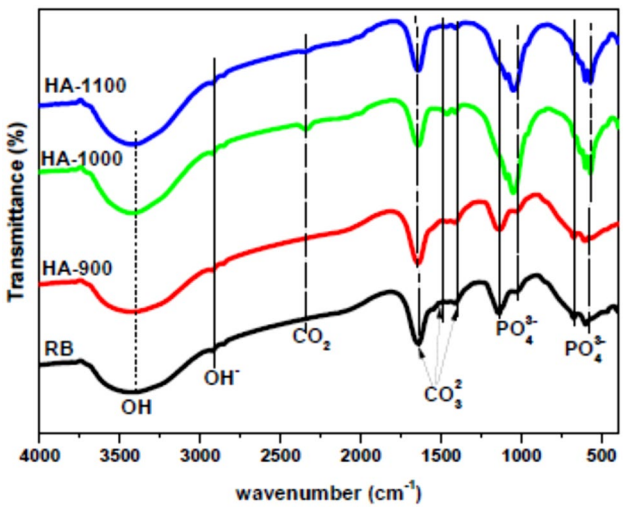

Fig. 14 FTIR of HAp at different temperatures [21]

about the conversion of calcium to phosphate into apatite. The FTIR (Fig. 14) figures exhibited the phosphate and hydroxyl crests in the heat-treated samples, which produced a characteristic elongating mode of O–H band at almost 3417 cm^{-1}, which is discernable in all the FTIR spectra of HAp.

Saber-Samandari et al. [92] used Micro-Raman Spectroscopy to show how the coating process affects the characteristics of hydroxyapatite. The HAp was sieved to a particle size of 30 ± 10 µm. Splats were heat-treated to crystallize any remaining amorphous phase. FTIR spectroscopy of the powder showed a clear hydroxyl vibration peak, at both 630 cm^{-1} and 3570 cm^{-1} (Fig. 15b). The second peak was located on a broad band between 2500 and 3600 cm^{-1}, showing asymmetrical and symmetrical extending vibrations of adsorbed water. The most intense absorption bands of hydroxyapatite were situated at 1029 cm^{-1} and 1092 cm^{-1}, matching to the asymmetric extending modes of $PO4^{3-}$, while the peaks at 961 and 471 cm^{-1} derived from the symmetric stretching and bending mode of $PO4^{3-}$, respectively, and this showed that Raman spectroscopy is more appropriate. The XRD of the powder showed a single-phase hydroxyapatite (Fig. 15a). The most concentrated hydroxyapatite (211) peak is located at 31.8 2θ.

Saber-Samandari et al. [93] studied, the morphology of solidified droplet "splats" using Scanning Electron Microscopy (SEM). The topography of splats sprayed onto substrates at room temperature (25 °C) and preheated to 100 °C and 300 °C was investigated (Fig. 16). The splat shape was found to be strongly dependent on substrate preheating temperature. A very early stage of re-crystallization was detected using Transmission Electron Microscopy (TEM) for splats deposited onto 300 °C preheated substrates. TEM in conjunction with Focused Ion Beam (FIB), revealed the splats' ultra-micro-structure. Splats deposited onto the substrate at 300 °C showed generally well- adherent inter faces. TEM dispersion (Fig. 17) in conjunction with Focused Ion Beam (FIB) (Fig. 18), revealed the splats' ultra-micro-structure.

Saber-Samandari & Gross [Q] characterized the deposits of calcium phosphate produced by thermal printing in terms of structure, topography and mechanical properties. Hydroxyapatite was molten and directed to (a) a titanium target in relative motion and (b) stationary titanium substrates preheated to 100 °C and 350 °C. Scanning electron microscopy showed round-like deposits, but high resolution profilometry measured the profile. Micro-Raman

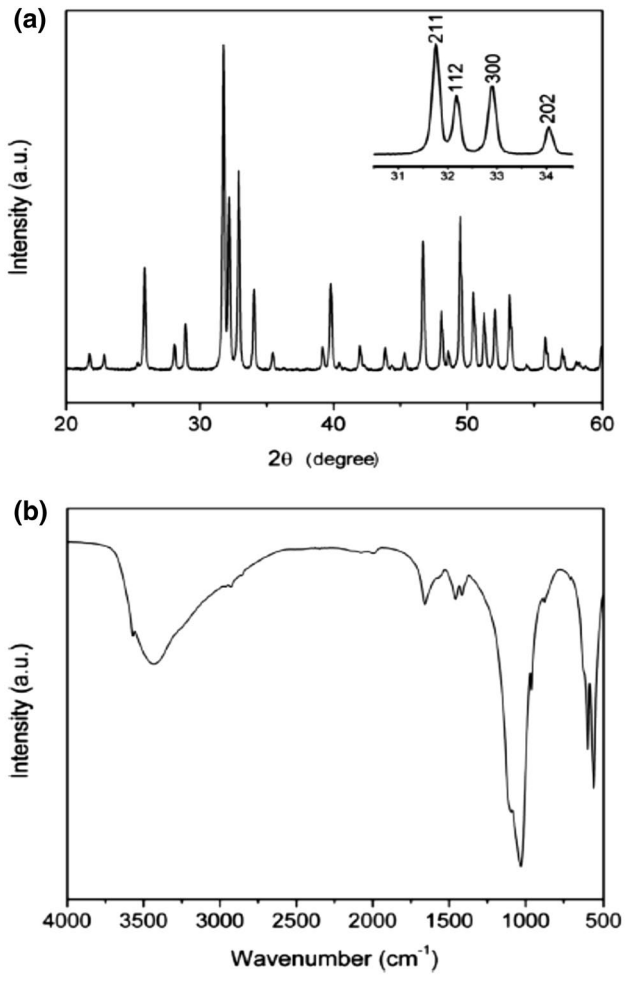

Fig. 15 Characterization of the starting powder with **a** XRD and **b** FTIR [92]

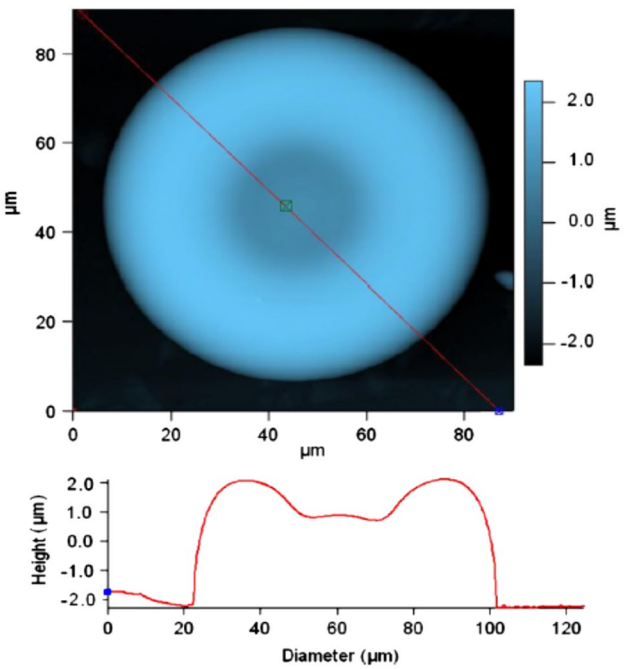

Fig. 16 FIB image of solidified CaP droplet splats [93]

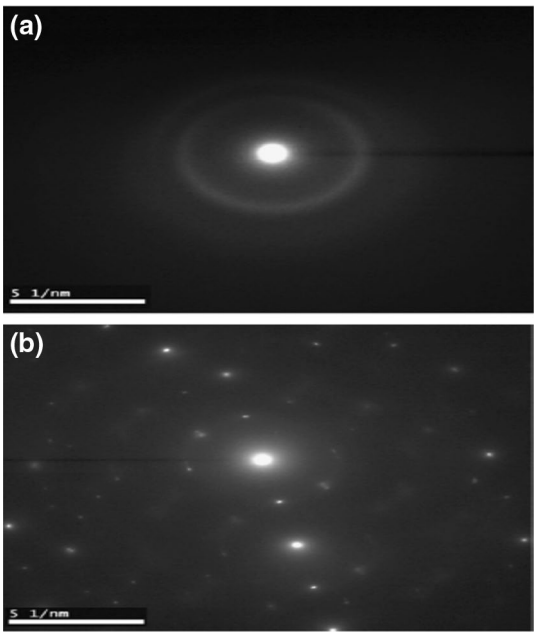

Fig. 17 Topographic image [93]

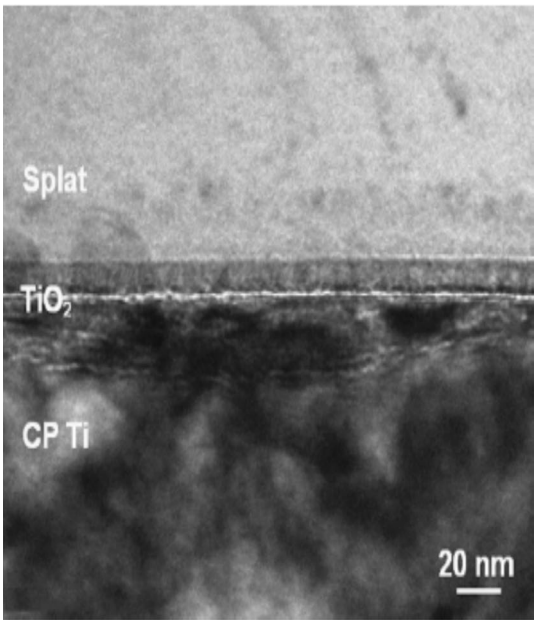

Fig. 18 Diffraction patterns (TEM) **a** a typical amorphous structure **b** re-crystallization stage [93]

spectroscopy and X-ray diffraction characterized the surface for structure. The characterization and testing approach is useful for hemispherical deposits produced by printing, coatings (laser ablation, thermal spraying, simulated body fluid) and melt extrusion elements in scaffolds.

4 Mechanical properties of hydroxyapatite

The mechanical properties of the composite biomaterials, HAp is the most alike to those of the human bone tissue [94, 95]. Therefore, their mechanical properties are of huge importance. Mechanical properties of some metals, ceramics and biomaterials classification are presented in Tables 3, 4 and 5 respectively. Also, some consideration in materials for biomedical application is shown in Table 6, while some organic and inorganic composite for biomedical application is given in Table 7. Among these biomaterials, hydroxyapatite is the most widely studied bioactive and biocompatible material. However, it has lower young's modulus and fracture toughness with brittle nature [21, 45, 96]. Hence, it is required to produce a biomaterial with good mechanical properties. As it relates to bio-ceramics, the mechanical properties that are of interest includes: Hardness testing, compressive strength evaluation, Fracture toughness testing, Young Modulus evaluation, Brittle index. Elastic modulus describes the stiffness of the bioceramic within the elastic range when tensile and compressive loads are applied [21, 96, 97]. The strength of bio-ceramics is an important mechanical property because they are brittle. Therefore, in this case, nano-indentation test is carried out to determine the elastic modulus of these nano materials. Hardness is quite important for comparing the properties of biomaterials. It is used for finding the suitability of the clinical importance and utilization of the biomaterials [96–102].

HAp in its bulk contains calcium and phosphate, having stoichiometric ratio 1.67 Ca/P. It has been determined that this ratio can effectively promotes bone regeneration [76]. Natural HAp in most cases does not give exact stoichiometric ratio due to the fact that the ratio is not chemically controlled. It also contains insufficient calcium or phosphorus [105]. Calcium position is the supreme vacancy in HAp, in which cations such as Na^{+}, Mg^{2+} and Al^{3+} are replaced on calcium position, while carbonate ion replaces phosphate or hydroxide ion, and fluoride ion can replace hydroxide ion [105].

Some requirements are needed in the classification of any material for biomedical applications. First, the material should have good biocompatibility, which means that the material should not be alien to the host organism. Second, the material should have high biodegradability, meaning that the materials should be harmlessly degraded in the host organism to restore natural functions. Third, the material should have mechanical integrity so that the load-bearing structure can be replaced. Currently, many types of ceramics (zirconia, bioglass, alumina and hydroxyapatite), metals and metal alloys are adopted for load-bearing applications. Such as dental

Table 3 Metals mechanical properties [134]

Biometals	Young's modulus (GPa)	Tensile strength (MPa)	Compressive strength (MPa)	Hardness (vickers, kg/mm)	Fatigue strength (MPa)
Ti	110	300–740	550	120–200	240
Ti-6Al-4 V alloy	120	860–1140	860	310	280–600
Stailess steel	190	500–950	600	130–180	260–280
Co-Cr alloy	210	665–1277	655	300–400	200–300

Table 4 Biomaterials mechanical properties [134]

Bioceramics	Young's modulus (GPa)	Tensile strength (GPa)	Compressive strength (GPa)	Fracture toughness (MPa $m^{1/2}$)	Hardness (HV)	Flexural strength (MPa)	Density (g/cm^3)	Bond strength (GPa)
Alumina	390	0.31	3.9	5.2	2000	390	3.9	300–400
Zirconia[b]	205	0.42	3	12	1150	1300	6	200–500
HA	80–110	0.05	0.4–0.9	0.7–1.2	600	37	3.16	120

[b]Partially stabilized Zirconia

replacements and replacements for bone connections or medical purposes [106]. Hence, biomaterials mechanical properties are essential most especially when applied in human load bearing area [107]. Among these biomaterials, hydroxyapatite (HAp) is the most widely studied biomedical material. An increasing research is geared towards its mechanical properties improvement because of it is brittle and low Young's modulus and fracture toughness [22, 26]. To the researcher, the mechanical properties design data sets the standard for the material or product [17, 71]. The heat treatment process and the working temperature can be used to alter the mechanical possessions. Some studies on the Ca/P ratio of HAp from different sources is shown Table 8 [108]. The present study intends to produce HAp from bovine and catfish bones before mixing them in different proportions (%wt) for further investigation to improve the mechanical properties of the produced HAp.

Amirhossein et al. [108] produced natural nanohydroxyapatite through calcination of raw turkey femur-bone waste powder at 850 °C after ball milling the powder. The compressive strength results (Fig. 19a) of 13.2, 24.23, 35.24, and 37.44 MPa were obtained at calcination temperatures of 850, 950, 1050, and 1150 °C, respectively. The highest strength value was gotten at a temperature of 1150 °C. Vickers micro-hardness data increased from 2 GPa up to a maximum of 3.2 GPa at sintering temperatures of 850–1150 °C (Fig. 19b). The results revealed that the strength and hardness of the samples increased by increasing the sintering temperature up to 1150 °C.

Chen et al. [107] viewed the consequence of sintering temperature on the microstructure, densification, grain size/boundary, calcium/phosphorus (Ca/P) of biocompatible hydroxyapatite (HAp) ceramics prepared by cold isostatic pressing, i.e. the influence of ion ratio and mechanical properties. It was observed that as the sintering temperature rose from 900 to 1200 °C, the mechanical hardness increased from 166 kgf/mm^2 (about 1.63 GPa) to 497 kgf/mm^2 (about 4.87 GPa) and started to decline at 1300 °C.

Aarthy et al. [113] produced HAp from goat bone. The goat bone sample was subjected to thermal analysis (Fig. 20) in order to ascertain its thermal behaviour. They sintered the Vickers hardness (HV) values of the HAp samples at different temperatures which increases with increase in sintering temperature. The initial HV value was calculated to be 164.3 MPa at 1100 °C (HAp1), and increases to 169.5 MPa at 1200 °C (HAp2), 245.3 MPa at 1300 °C (HAp3) and lastly scopes the maximum of 301.3 MPa at 1400 °C (HAp4) (Fig. 21).

Foroughi et al. [114] produced HAp powder from bovine bones by heat treatment at 900 °C. Then he used the polyurethane squeegee duplication method to produce HAp scaffolds. In order to upturn the mechanical possessions of the stent, poly-3-hydroxybutyrate (P3HB) was coated on the stent for 30 s and 1 min. The compressive strength and moduli of the scaffold obtained with 50 wt% HAp are 1.46 and 21.27 MPa, respectively, which makes it suitable for biomedical engineering applications. Chang et al. [115] introduced nano-hydroxyapatite (nHAp) into a chitin and the result was dissolved in NaOH/urea aqueous solution at little temperature. He then prepared a new hybrid hydrogel, and considered its compressive strength. The compressive strength of the chitin/nHAP hybrid hydrogel (gel 2) was 274 kPa, which is higher than

Table 5 Biomaterials classification for bone grafting [134]

Biomaterials	Advantages[b]	Disadvantages	Applications	Examples
Metal and alloy	Too strong, tough, ductle	Dense, may corrode	Bone plates, loadbearing bone implants, dental arc wire and dental brackets	Titanium, stailess steel, Co-Cr alloys and Ti alloys
Ceramic	Bioinert	Brittle, poor tensile, low toughness, lack of resilience	Hip joints and loadbearing bone implants, Bone filler, coating on bio-implants, orbital implant, alveolar ridge augmentation, and bone tissue engineering	HA, bioglass, TCP
Polymer	Flexible, resilient, surface modifiable, selection of chemical functional groups	Not strong, toxic of a few degraded products	Bone tissue scaffolds, bone screws pins, bone plates, bone and dental filler, and bone drug delivery	Collagen, gelatin, chitosan, alginate, PLA, PGA, PLGA, PCL, PMMA, PE
Composite	Strong, design flexibility, enhanced mechanical reliability than monolithic	Properties might be varied with respect to fabrication methodology	Bone graft substitutes, middle ear implants, bone tissue scaffolds, guided bone regenerative membranes, and bone drug delivery	HA/collagen, HA/gelatin, HA/alginate, HA/PLGA, HA/PLLA, HA/PE
Nanocomposite	Larger surface area, high surface reactivity, relatively strong interfacial-bonding, design flexibility, enhanced mechanical reliability than monolithic and/or microcomposite	No optimized technique for material processing	Major areas of orthopedics, tissue engineering, and drug delivery	Nano-HA/collagen, Nano-HA/gelatin, Nano-HA/chitosan, Nano-HA/PLLA

[b]Common characteristics of biomaterials like biocompatibility

Table 6 Considerations for materials selection [104]

Factors	Description		
1st Level material properties	Chemical/biological characteristics Chemical composition (bulk and surface)	Physical Characteristics Density	Mechanical/Structural characteristics Elastic modulus Poisson's ratio Yield strength Tensile strength Compressive strength
2nd Level material properties	Adhesion	Surface topology (texture and roughness)	Hardness Shear modulus Shear strength Flexural modulus Flexural strength
Specific functional requirements (based on application)	Biofunctionality (non-thrombogenic, cell adhesion, etc.) Bioinert (non-toxic, non-irritant, non-allergic, non-carcenogenic, etc.) Bioactive Biostability (resistant to corrosion, hydrolysis, oxidation, etc.) Biogradation	Form (solid, porous, coating, film, fiber, mesh, powder) Geometry Coefficient of thermal expansion Electrical conductivity Color, aesthetics Refractive index Opacity or translucency	Stiffness or rigidity Fracture toughness Fatigue strength Creep resistance Friction and wear resistance Adhesion strength Impact strength Proof stress Abrasion resistance
Processing and fabrication	Reproducibility, quality, sterilization,	Packaging, secondary processability	

Characteristics of host: tissue, organ, species, age, sex, race, health condition, activity, systemic response

Medical/surgical procedure, period of application/usage

Cost

Table 7 Scaffolds for biomedical uses

Inorganic/organic composites or scaffolds	Applications	References
HAp with collagen Scaffold	Bone graft materials, drug delivery and tissue engineering	[96, 98]
HAp/gelatin composite	Drug delivery, skin tissue regeneration and bone tissue engineering	[99]
HAp-chitosan composite	Antibacterial, bone tissue engineering and drug delivery	[100]
HAp and platel-rich Fibrin scaffold	Bone tissue regenerative, wound dressing and gene delivery	[101]
Hap/cellulose composite	Bone tissue engineering, water purification and biomedical applications	[102]
HAp/alginate composite	Bone tissue engineering and drug delivery	[97]

Table 8 Ca/P ratios of other studies

HAp Source	Ca/P	Sintering temperature (°C)	References
Pig bones	1.94	1050	[109]
Cortical bovine bones	1.7	1100	[110]
Bovine bones	1.65	750	[111]
Bovine bones	1.58	1000	[112]
Catfish bone	1.58	900	[45]
Turkey bone	1.63	1150	[108]

that of the chitin hydrogel. Baradaran et al. [116] used a simple hydrothermal method to synthesize hydroxyapatite (HA)-graphene nanosheets (GNs) composite system in situ. It was observed that the reduced graphene oxide (rGO) enhanced hydroxyphosphorus Greystone nanotube (nHA) composite material. The amalgamation route was executed by hot isostatic persuasive (HIP) at 160 MPa. He studied the microhardness of 0 wt%, 0.5 wt%, 1 wt% and 1.5 wt% of the reduced graphene oxide (rGO) hydroxyapatite (HAp)-graphene nanosheets (GNs). He recorded the microhardness values (MPa) of (322 ± 8), (363 ± 5), (425 ± 4), (381 ± 7); and the fracture toughness (GPa) of (0.81 ± 0.05), (0.95 ± 0.03), (1.31 ± 0.07) and (1.51 ± 0.05), respectively.

Kim et al. [117] shaped a chitosan composite scaffold with great strength and controllable pore structure through uniformly isolated nano-sized hydroxyapatite powder (HAp content increased to 70 wt%). The compressive strength

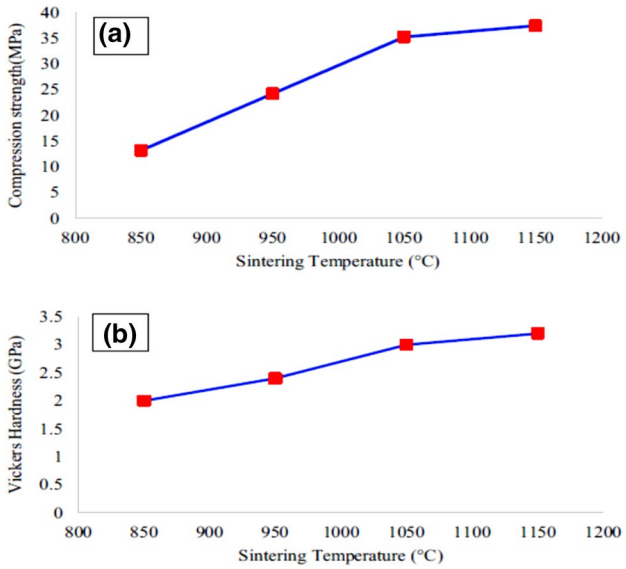

Fig. 19 Values for: **a** Compressive strength **b** Vickers hardness [108]

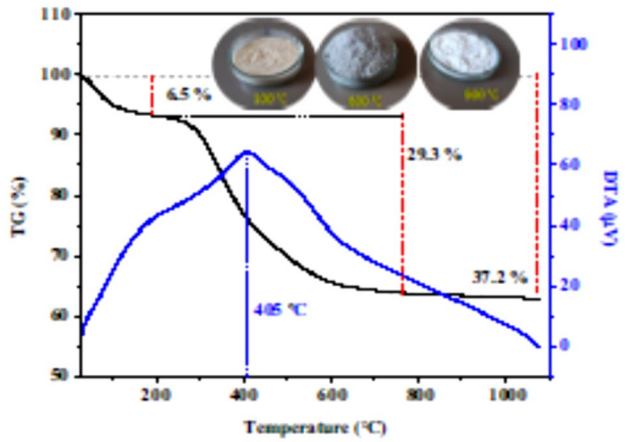

Fig. 20 The TGA of raw goat bone [113]

of alginate/chitosan was 0wt. The% of hydroxyapatite was 0.27 MPa and 70 wt%. Yazdanpanah et al. [118] looked at the production and sintering of hydroxyapatite composite materials with different weight percentages of soda lime glass. The sintering was meant to improve its mechanical properties. The compressive strengths of 0% glass, 2.5% glass and 5% glass were (32.46 ± 2.01) (40.61 ± 5.7) and (43.03 ± 1.42) MPa, respectively. Harabi et al. [119] added altered percentages of B_2O_3 (0.5–5.0 wt%) to NHA powder to stimulate densification. He reduced the sintering temperature of porous NHA. After that, the powder was uniaxially cold pressed at 75 MPa and sintered at 1050 °C for 2 h. The best Vickers microhardness value was 2.1 GPa. A bending strength of about 57 MPa was also obtained using the projected method.

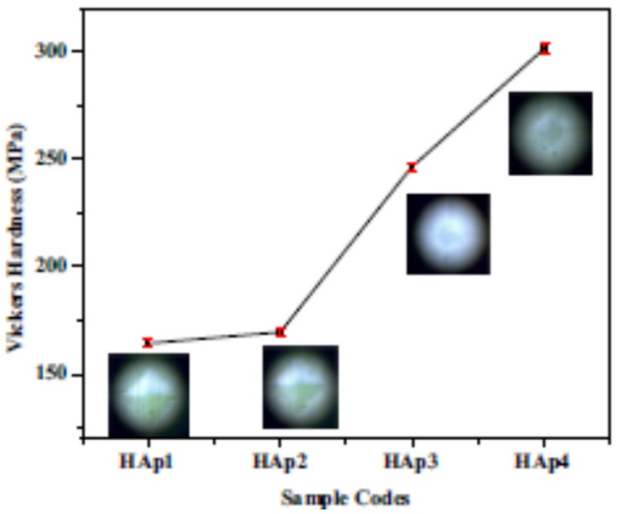

Fig. 21 Vickers hardness of sintered samples [113]

Table 9 Young modulus and fracture toughness [121]

Orientation	H (GPa)	E_r (GPa)	E (GPa)	K_{IC} (MPam$^{1/2}$)
Side	6.41	137.98	143.56	0.45
Base	7.06	142.92	150.38	0.35

Obada et al. [120] executed a laboratory study on the mechanical properties of kaolin reinforced hydroxyapatite (K-HAp) made from animal osteo under varied sintering conditions. HAp particles were produced by a simple heat treatment way and reinforced with 15 wt% selected kaolin (HAp/15 wt% BK) using sol–gel means to mix them. The HAp and K-HAp-derived scaffolds are made by cold pressing at a compaction pressure of 500 Pa. In open air, the stent was sintered at 900 °C, 1000 °C and 1100 °C for a residence time of 2 h, and its mechanical properties was studied. At the supreme sintering temperature (1100 °C), the hardness of the bracket was 0.93 and 1.09 GPa. Under the compaction pressure of 500 Pa, the compressive strength of KHAp was 7.84 MPa, and the compressive strength of non-reinforced HAp matrix was 0.69 MPa. The research results proved that the mechanical properties of the synthetic kaolin-enhanced HAp are suitable for human trabecular bones compared to the scaffold produced at a low pressure of 500 Pa.

Saber-Samandari and Gross [121] studied the micromechanical properties of single crystal hydroxyapatite by nanoindentation (at the base and side) to investigate the hardness, elastic modulus and fracture toughness of the trivial samples. The hardness and elastic modulus were measured using the standard method projected by Oliver and Pharr [122]. The hardness and elastic modulus figures obtained revealed greater figures for the base (7.1

and 150.4 GPa) compared to the side (6.4 and 143.6 GPa) (Table 9). Fracture toughness was measured as 0.45 ± 0.09 and 0.35 ± 0.06 MPa $m^{1/2}$ for the side and base plane, respectively. The load at which cracking starts, showed prior crack development on the base (at 8 mN) related to the side (at 11 mN).

Saber-Samandari and Gross [123] in another study observed the crack resistance of Amorphous calcium phosphate (ACP) to assist know its activity in organic creatures and help in the proposal of CaP-based implants by satiating droplets to formulate a bulk sample and separate splats. The result proved that ACP has a lesser hardness and elastic modulus than HAp. Fracture toughness was established for fused silica (FS) to authenticate the method. In the experiment, a value of 0.6 ± 0.1 MPa $m^{1/2}$ was gotten for FS, whereas for the Sintered HAp (0.2 µm grain size) a fracture toughness of 0.9 ± 0.1 MPa $m^{1/2}$ was obtained. Likened to splats on the non-preheated substrate, a splat on the 100 °C preheated substrate has a lower toughness (0.31 ± 0.06 MPa $m^{1/2}$), and an even lower figure on the 350 °C substrate (0.17 ± 0.04 MPa $m^{1/2}$), Fig. 22.

Joneidi et al. [125] with space holder approaches conducted an experiment on bio-nanocomposite scaffold (BS). The response of the bio-nanocomposites buckle under load was examined with the aid of an Abaqus software. The results showed (Fig. 23) that the sample containing 15 wt% additives exhibited preferred mechanical property than the sample without additives. Similarly, the elastic modulus of the specimens rises twice with the introduction of additive (from 60 to 145 MPa). Likewise, the scaffold bio-nanocomposite did not come back to its unique state due to the elasticity of the ceramics and its deformation at the plastic region which was permanent and irreversible.

Obada et al. designed strontium (Sr) doped HAp through solution combustion. A low compaction pressure system was used for pelletizing the powders (Sr-HAp) to assess the physical and mechanical properties of the

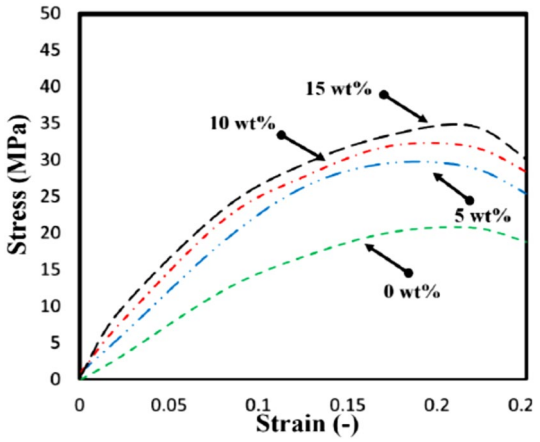

Fig. 23 Stress–strain plot of BS [125]

pellets. The hardness and fracture toughness were 0.38 GPa and 0.82 MPa $m^{1/2}$ and 0.20 GPa and 0.67 MPa $m^{1/2}$ for the doped and undoped Sr-HAp respectively. The SEM images suggested that strontium co-existed with the calcium ion in hydroxyapatite due to the presence of irregular bead like structures on a micro-scale. The Sr-HAp pellets were stable in Phosphate Buffer Saline solution [126].

Yang et al. [127] fabricated a novel co-dispersed Fe_3O_4–GO nanosystem through electrostatic self-assembly of positively charged Fe_3O_4 (pFe_3O_4) on negatively charged GO nanosheets. Afterward, the nanosystem was fused into poly L-lactic acid (PLLA) scaffolds constructed by means of selective laser sintering. Additionally, the nanosystem also revealed a harmonious improvement result on the mechanical properties of scaffolds, since the pFe_3O_4 loaded on GO enhanced the effectiveness of stress transfer in matrix. The tensile stress and compressive strength of scaffolds were increased by 67.1% and 132%, respectively (Fig. 24a). The tensile stress and strain

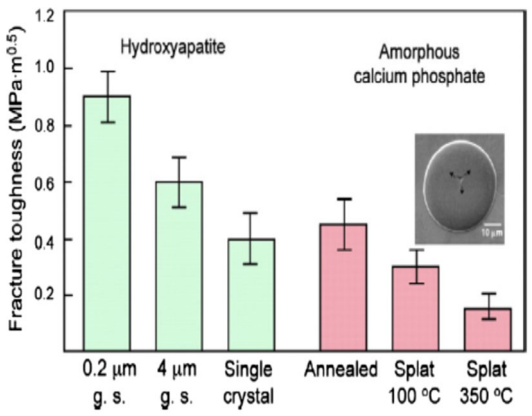

Fig. 22 Mechanical behavior of a single splat [123, 124]

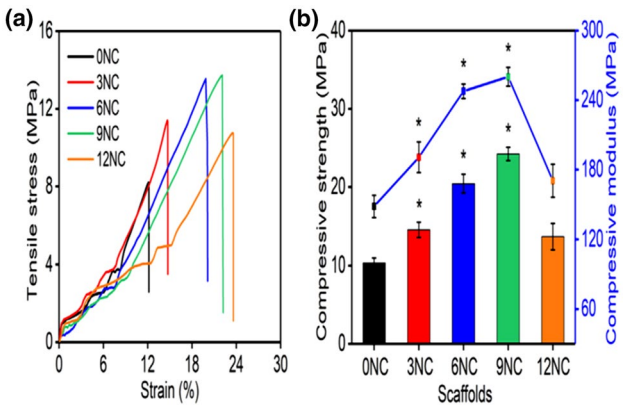

Fig. 24 **a** Tensile stress- strain **b** Compressive strength—of a scaffold [127]

of the 0NC scaffold was 8.2 MPa and 12.1%, respectively (Fig. 24a).

Shuai et al. produced a mace-like nanosystem to advance their dispersion by in-situ development of Ag nanoparticles on cellulose nanocrystal (CNC@Ag-NS) and was later added into poly-L-lactide (PLLA) scaffolds. A homogeneously dispersed result was observed in the scaffold. Promisingly, the mechanical properties of the scaffolds were strongly higher than that of PLLA/CNC scaffolds, owing to the mace-like CNC@Ag nanosystem improved the load transfer efficiency in the scaffold [128].

5 Physical properties of hydroxyapatite

The integrity of HAp can be assessed based on its mechanical (as discussed above) and physical properties (density and porosity). The slope of mechanical characteristics for sintered HAp differs in density and strain [129–131]. Though mechanical reliability is vital, porosity of scaffolds is equally a serious influence. It is so because, porosity marks the transfer of nutrients, metabolic wastes, etc. in cell culture [132]. Basically, microstructures of HAp are shaped by a bunch of defectiveness which have different forms, dimensions and porosity [120]. Some of the physical properties of HAp are shown in Table 10 below, while Table 11 displays the bio mechanical properties of bone. It has been formerly stated that porosities in the range of 40–90% supports osteointegration on the implant surface and boosted bond of implants with bone [133].

Table 10 Physical properties of HAp [134]

Properties	Experimental data
Chemical composition	$Ca_{10}(PO_4)_6(OH)_2$
Ca/P molar	1.67
Crystal system	Hexagonal
Space group	$P6_3/m$
Cell dimension (Å)	a = b = 9.42, c = 6.88
Young's modulus (GPa)	80–110
Elastic modulus (GPa)	114
Compressive strength (MPa)	400–900
Bending strength (MPa)	115–200
Density (g/cm^3)	3.16
Relative density (%)	95–99.5
Fracture toughness (MPa m$^{1/2}$)	0.7–1.2
Hardness (HV)	600
Decomposition temperature (°C)	> 1000
Melting point (°C)	1614
Dielectric constant	7.40–10.47
Thermal conductivity (W/cm K)	0.013
Biocompatibility	High
Bioactivity	High
Biodegradation	Low
Cellular-compatibility	High
Osteoinduction	Nil
Osteoconduction	High

Table 11 Properties of bone [134]

Properties	Measurements	
	Cortical bone	Cancellous bone
Young's modulus (GPa)	14–20	0.05–0.5
Tensile strength (MPa)	50–150	10–20
Compressive strength (MPa)	170–193	7–10
Fracture toughness (MPa m$^{1/2}$)	2–12	0.1
Strain to failure	1–3	5–7
Density (g/cm^3)	18–22	0.1–1.0
Apparent density (g/cm^3)	1.8–2.0	0.1–1.0
Surface/bone volume (mm^2/mm^3)	2.5	20
Total bone volume (mm^3)	1.4×10^6	0.35×10^6
Total internal surface	3.5×10^6	7.0×10^6

Joneidi et al. [125] produced a porous scaffold for bone substitute using space holder methods. It was observed that the specimen without additive brought down the porosity value because of rise it the mass percentage of the metallic stage. Correspondingly, the porosity of the specimens was in the range of 70–80%. Equally, Table 12 showed that as the MNPs was introduced to the based bioceramics the Poisson Ratio rises alike to the density value.

Obada et al. [120] produced HAp from Bovine bone. With Eq. 1 below, the the density of HAp determined, using 3.16 g/cm^3 as the theoretical density of HAp [20, 135, 136].

$$\text{Porosity}\ (\%) = \left(1 - \frac{\textit{Weight of HAp}}{\textit{Volume of HAp} \times \textit{Density of HAp}}\right) \times 100 \quad (1)$$

$$\text{Density}\ (\text{g/cm3}) = \frac{\textit{mass}}{\textit{volume}} \quad (2)$$

From the result, it was observed that the porosity (which varied from 46.9 ± 0.10 to 60.2 ± 0.76%) of sintered samples decreased with rising in sintering temperature.

Table 12 Porous scaffold density and poisson ratio [125]

Materials (wt%)	Density (g/cm^3)	Elastic modulus (MPa)	Poisson ratio
0	3.2	60 ± 5	0.30
5	3.5	85 ± 5	0.30
10	3.2	110 ± 5	0.32
15	3.3	145 ± 5	0.34

Yang et al. [137] examined a novel nanophase ceramic for improved drug transporter. With space holder technique, the bulk of the study was the proposal of the scaffold to produce a plan with suitable porosity in the array of 70–85% alongside acceptable compressive strength, that was estimated by the scope of the cavity, bending properties, fusion of magnetite nanoparticles, porosity and rate of degradability.

6 Summary

A careful attention from different researches exposes the process of extracting HAp from bovine or catfish bone, standard methods of testing the mechanical properties and characterization techniques that guarantee acceptable HAp with improved mechanical and physical properties. This is shown in Fig. 4. Note that the cost of electricity tariff (62.33 Naira per kwh) in Nigeria today discourages the pretreatment process used by Abifarin et al. [21] and Obada et al. [22, 120] as this will increase the cost of producing natural hydroxyapatite in large quantity. Therefore, burning in open with charcoal will bring down the cost of producing hydroxyapatite. It was observed that HAp can have a hexagonal shape. Also, HAp is brittle in nature, but its biodegradable characteristics makes it suitable for biomedical application [73].

7 Conclusion

Hydroxyapatite (HAp) with good mechanical properties are of great use and important applications in dentistry and orthopedic for biomedical engineering. This review paper chiefly ezzmphases on the use of bovine and catfish wastes to extract HAp. In this paper, the production steps of HAp from bovine and catfish wastes were classified as follows: soaking the bio-wastes in water, washing, boiling for hours, oven drying at certain temperature (example 150 °C), thermal stability analysis, calcination, crushing with mortar and pestle, and sieving with a sieve. The mechanical testing and characterization come and the above steps. Apatites have arrangements and properties comparable to human bones. In this review, there is a discussion on the treatment methods capable of producing hydroxyapatite with the desired mechanical and physical characteristics for the applications in tissue engineering scaffolds for bone implants. It was observed that the calcination method can convert HAp into other calcium phosphate phases, such as β-TCP, at high temperatures. However, it is concluded that the alkaline heat treatment methods, ionic liquid pretreatment and enzymatic hydrolysis methods produce pure phase HAp, but have lower crystallinity matched to the calcination routine. Record of the procedures used in this review study can produce nano-scale HAp with altered morphologies. The standard values for tensile strength were found to be within the range of 40–300 MPa, compressive strength was 400–900 MPa, while Elastic modulus was 80–120 GPa and fracture toughness was 0.6–1 $MPa{\cdot}m^{1/2}$ [20, 135, 136]. Also, the porosity range was 70–85% [138], density is 3.16 g/cm^3 and relative density is 95–99.5% [20, 71, 95, 104, 136, 138–145]. The literature revealed that CaP ratio varies in relation to the source and sintering temperature. For example, for bovine bone, a CaP ratio of 1.7 [110] and 1.65 [111] was obtained at 1100 °C and 750 °C respectively. The inference is that if the main parameters of natural HAp (NHA) fabrication such as compaction pressure, sintering temperature and sintering residence time are carefully controlled, they may lead to mechanical enhancement of NHA-based bioceramics. It is desirable to make full use biogenic materials to derive HAp with optimal properties and proper synthesis methods in producing HAp for application tissue engineering to meet the increasing clinical requirements. With good technique, the mechanically and enzymatically treated fish bone apatite yielded higher dissolved organic carbon (DOC) and biochemical oxygen need (BON) concentrations than those produced by thermal treatments.

Acknowledgements I wish to appreciate the maximum support received from Professor Solomon Chuka Nwigbo and Engineer Johnson K. Abifarin for their knowledge of synthesis of hydroxyapatite and their inspiration to organise this review. I, OA Osuchukwu acknowledges the knowledge exposed and support given at this stage in synthesis of hydroxyapatite under the leadership of Dr David Obada of Ahmadu Bello University, Zaria.

Author contributions Professor AS and Professor IA are the supervisors of the work, while OOA, BA and CSN were researcher, reviewer and reader respectively. We all contributed immensely.

Data availability Since this is a review paper, the data and materials presented in this manuscript were sourced from different researches done on Hydroxyapatites production and all References are given.

Declarations

Conflict of interest We, the authors of the manuscript titled "Synthesis and Mechanical Properties Investigation of Natural Derived Hydroxyapatite Scaffolds for Bone Implants: A Review", hereby wish to submit the manuscript for your kind attention. We hereby declare no conflict of interest.

Consent to participate All authors play their specific roles for the success of this manuscript.

Consent for publication We the authors of this manuscript fully give our consent for publication in your journal.

References

1. Giannoudis PV, Dinopoulos H, Tsiridis E (2005) Bone substitutes: an update. Injury 36(3):S20–S27
2. Farazin A, Aghdam HA, Motiffard M, Aghadavoudi F, Kordjamshidi A, SaberSamandari S, Khandan A (2019) A polycaprolactone bio-nanocomposite bone substitute fabricated for femoral fracture approaches: molecular dynamic and micromechanical Investigation. J Nanoanaly 6(3):172–184
3. Khandan A, Ozada N, Saber-Samandari S, Nejad MG (2018) On the mechanical and biological properties of bredigite-magnetite (Ca7MgSi4O16-Fe3O4) nanocomposite scaffolds. Ceram Int 44(3):3141–3148
4. Monshi M, Esmaeili S, Kolooshani A, Moghadas BK, Saber-Samandari S, Khandan A (2020) A novel three-dimensional printing of electroconductive scaffolds for bone cancer therapy application. Nanomed J 7(2):138–148
5. Heydary HA, Karamian E, Poorazizi E, Heydaripour J, Khandan A (2015) Electrospun of polymer/bioceramic nanocomposite as a new soft tissue for biomedical applications. J Asian Ceram Soc 3(4):417–425
6. Khandan A, Ozada N (2017) BredigiteMagnetite (Ca7MgSi4O16-Fe3O4) nanoparticles: a study on their magnetic properties. J Alloy Compd 726:729–736
7. Ghayour H, Abdellahi M, Nejad MG, Khandan A, Saber-Samandari S (2018) Study of the effect of the Zn2+ content on the anisotropy and specific absorption rate of the cobalt ferrite: the application of Co 1–x Zn x Fe2O4 ferrite for magnetic hyperthermia. J Aust Ceram Soc 54(2):223–230
8. Rad AS, Samipour V, Movaghghar NS, Mirabi A, Shahavi MH, Moghadas BK (2019) X12N12 (X= Al, B) clusters for protection of vitamin C; molecular modeling investigation. Surf Interfaces 15:30–37
9. Khandan A, Jazayeri H, Fahmy MD, Razavi M (2017) Hydrogels: types, structure, properties, and applications. Biomat Tiss Eng 4(27):143–169
10. Hashemi SA, Esmaeili S, Ghadirinejad M, Saber-Samandari S, Sheikhbahaei E, Kordjamshidi A, Khandan A (2020) MicroFinite element model to investigate the mechanical stimuli in scaffolds fabricated via space holder technique for cancellous bone. ADMT J 13(1):51–58
11. Burg KJ, Porter S, Kellam JF (2000) Biomaterial developments for bone tissue engineering. Biomaterials 21(23):2347–2359
12. Dorozhkin SV, Epple M (2002) Biological and medical significance of calcium phosphates. Angew Chem Int Ed 41(17):3130–3146
13. Sahmani S, Shahali M, Nejad MG, Khandan A, Aghdam MM, SaberSamandari S (2019) Effect of copper oxide nanoparticles on electrical conductivity and cell viability of calcium phosphate scaffolds with improved mechanical strength for bone tissue engineering. Eur Phys J Plus 134(1):7
14. Khandan A, Karamian E, Bonakdarchian M (2014) Mechanochemical synthesis evaluation of nanocrystalline bone derived bioceramic powder using for bone tissue engineering. Dent Hypotheses 5(4):155
15. Laonapakul T (2015) Synthesis of hydroxyapatite from biogenic wastes. Eng Appl Sci Res 42(3):269–275
16. Engstrand UJ, Persson C, Engqvist H (2015) Evaluation of methods to determine the porosity of calcium phosphate cements. J Biomed Mater Res Part B Appl Biomater 103(1):62–71
17. Bukawa H (2006) The engineering of craniofacial tissues in the laboratory: a review of schaffolds of biomaterials and implants coatings. Dent Clin N Am 50:205–216
18. Ross MD, Hadzik J, Kozak K, Kamil J, Gerber H, Dominiak M, Kunert-Keil C (2017) New nano-hydroxyapatite in bone defect regeneration: a histological study in rats. Ann Anat—Anat Anz 213:83–90
19. Farokhi M, Mottaghitalab F, Samani S, Shokrgozar MA, Kundu SC, Reis RL, Kaplan DL (2018) Silk fibroin/hydroxyapatite composites for bone tissue engineering. Biotechnol Adv 36(1):68–91
20. Ramesh S, Loo ZZ, Tan CY, Chew WK, Ching YC, Tarlochan F, Sarhan AA (2018) Characterization of biogenic hydroxyapatite derived from animal bones for biomedical applications. Ceram Int 44(9):10525–10530
21. Abifarin JK, Obada DO, Dauda ET, Dodoo-Arhin D (2019) Experimental data on the characterization of hydroxyapatite synthesized from biowastes. Data Brief 26:104485
22. Obada DO, Dauda ET, Abifarin JK, Dodoo-Arhin D, Bansod ND (2020) Mechanical properties of natural hydroxyapatite using low cold compaction pressure: Effect of sintering temperature. Mater Chem Phys 239:122099
23. de Groot K (1980) Bioceramics consisting of calcium phosphate salts. Biomaterials 1:47–50
24. Figueiredo M, Fernando A, Martins G, Freitas J, Judas F, Figueiredo H (2010) (2010) Effect of the calcination temperature on the composition and microstructure of hydroxyapatite derived from human and animal bone. Ceram Int 36(8):2383–2393
25. Ramesh S, Tolouei R, Hamdi M, Purbolaksono J, Tan YC, Amiriyan M, Teng WD (2011) Sintering behavior of nanocrystalline hydroxyapatite produced by wet chemical method. Curr Nanosci 7(6):845–849
26. Ramesh S, Aw KL, Tolouei R, Amiriyan M, Tan CY, Hamdi M, Teng WD (2013) Sintering properties of hydroxyapatite powders prepared using different methods. Ceram Int 39(1):111–119
27. Tan CY, Yaghoubi A, Ramesh S, Adzila S, Purbolaksono J, Hassan MA, Kutty MG (2013) Sintering and mechanical properties of MgO-doped nanocrystalline hydroxyapatite. Ceram Int 39(8):8979–8983
28. Kamalanathan P, Ramesh S, Bang LT, Niakan A, Tan CY, Purbolaksono J, Teng WD (2014) (2014) Synthesis and sintering of hydroxyapatite derived from eggshells as a calcium precursor. Ceram Int 40(10):16349–16359
29. Brzezińska-Miecznik J, Haberko K, Sitarz M, Bućko MM, Macherzyńska B (2015) Hydroxyapatite from animal bones–extraction and properties. Ceram Int 41(3):4841–4846
30. Niakan A, Ramesh S, Tan CY, Purbolaksono J, Chandran H, Teng WD (2015) Effect of annealing treatment on the characteristics of bovine bone. J Ceram Process Res 16(2):223–226
31. Niakan A, Ramesh S, Naveen SV, Mohan S, Kamarul T (2017) Osteogenic priming potential of bovine hydroxyapatite sintered at different temperatures for tissue engineering applications. Mater Lett 197:83–86
32. Niakan A, Ramesh S, Ganesan P, Tan CY, Purbolaksono J, Chandran H, Teng WD (2015) Sintering behaviour of natural

porous hydroxyapatite derived from bovine bone. Ceram Int 41(2):3024–3029
33. Goto T, Sasaki K (2014) Effects of trace elements in fish bones on crystal characteristics of hydroxyapatite obtained by calcination. Ceram Int 40(7):10777–10785
34. Pal A, Paul S, Choudhury AR, Balla VK, Das M, Sinha A (2017) Synthesis of hydroxyapatite from lates calcarifer fish bone for biomedical applications. Mater Lett 203:89–92
35. Ramirez-Gutierrez CF, Londoño-Restrepo SM, Del Real A, Mondragón MA, Rodriguez-García ME (2017) Effect of the temperature and sintering time on the thermal, structural, morphological, and vibrational properties of hydroxyapatite derived from pig bone. Ceram Int 43(10):7552–7559
36. Ramesh S, Natasha AN, Tan CY, Bang LT, Ching CY, Chandran H (2016) Direct conversion of eggshell to hydroxyapatite ceramic by a sintering method. Ceram Int 42(6):7824–7829
37. Edralin EJM, Garcia JL, dela Rosa FM, Punzalan ER (2017) Sonochemical synthesis, characterization and photocatalytic properties of hydroxyapatite nano-rods derived from mussel shells. Maters Lett 196:33–36
38. Wu SC, Hsu HC, Hsu SK, Tseng CP, Ho WF (2017) Preparation and characterization of hydroxyapatite synthesized from oyster shell powders. Adv Powder Technol 28(4):1154–1158
39. Stea S, Visentin M, Savarino L, Donati ME, Pizzoferrato A, Moroni A, Caja V (1995) Quantitative analysis of the bone-hydroxyapatite coating interface. J Mater Sci: Mater Med 6(8):455–459
40. Lu L, Mikos AG (1996) The importance of new processing techniques in tissue engineering. MRS Bull 21(11):28–32
41. Beaufils S, Rouillon T, Millet P, Le Bideau J, Weiss P, Chopart JP, Daltin AL (2019) Synthesis of calcium-deficient hydroxyapatite nanowires and nanotubes performed by template-assisted electrodeposition. Mater Sci Eng, C 98:333–346
42. Foroutan S, Hashemian M, Khandan A (2020) A novel porous graphene scaffold prepared using freeze-drying technique for orthopedic approaches: fabrication and buckling simulation using GDQ method. Iran J Mater Sci Eng 17(4):62–76
43. Shi X, Wang Y, Jia R, Liu F, Zhang J (2019) Experimental investigations on microstructures and mechanical properties of white yak horns sheath. Results Phys 13:s102174. https://doi.org/10.1016/j.rinp.2019.102174
44. Gross KA, Saber-Samandari S, Heemann KS (2010) Evaluation of commercial implants with nanoindentation defines future development needs for hydroxyapatite coatings. J Biomed Mater Res Part B: Appl Biomater: An Off J Soc Biomater, Jpn Socr Biomater, Aust Soc Biomater Korean Soc Biomater 93(1):1–8
45. Akpan ES, Dauda M, Kuburi LS, Obada DO, Dodoo-Arhin D (2020) A comparative study of the mechanical integrity of natural hydroxyapatite scaffolds prepared from two biogenic sources using a low compaction method. Results Phys. https://doi.org/10.1016/j.rinp.2020.103051
46. Akpan ES, Dauda M, Kuburi LS, Obada DO (2021) Box-Behnken experimental design for the process optimization of catfish bones derived hydroxyapatite: a pedagogical approach. Mater Chem Phys 272:124916
47. Iranmanesh P, Abedian A, Nasri N, Ghasemi E, Khazaei S (2014) Stress analysis of different prosthesis materials in implantsupported fixed dental prosthesis using 3D finite element method. Dent Hypotheses 5(3):109
48. Hasheminia D, Razavi SM, Nazari H, Khazaei S, Soleimanzadeh P (2018) Systemic supplement with resveratrol increased bone formation in ratsâ alveolar socket Aumento de la formaciÃ3n Ã3sea en el hueso alveolar de rata con suplemento sistÃ© mico con resveratrol. Int J Morphol 36(2):391–394
49. Gao C, Feng P, Peng S, Shuai C (2017) Carbon nanotube, graphene and boron nitride nanotube reinforced bioactive ceramics for bone repair. Acta Biomater 61:1–20
50. Shuai C, Gao C, Feng P, Peng S (2014) Graphene-reinforced mechanical properties of calcium silicate scaffolds by laser sintering. RSC Adv 4(25):12782–12788
51. White AA, Best SM, Kinloch IA (2007) Hydroxyapatite–carbon nanotube composites for biomedical applications: a review. Int J Appl Ceram Technol 4(1):1–13
52. Touri R, Moztarzadeh F, Sadeghian Z, Bizari D, Tahriri M, Mozafari M (2013) The use of carbon nanotubes to reinforce 45S5 bioglass-based scaffolds for tissue engineering applications. BioMed Res Int. https://doi.org/10.1155/2013/465086
53. Ito Y, Hasuda H, Kamitakahara M, Ohtsuki C, Tanihara M, Kang IK, Kwon OH (2005) A composite of hydroxyapatite with electrospun biodegradable nanofibers as a tissue engineering material. J Biosci Bioeng 100:43–49. https://doi.org/10.1263/jbb.100.43
54. Afonso AS (1998) Interaction between biomaterials and bone tissue. 213f. Thesis (PhD) school of dental medicine, University of Porto, Porto, Portugal
55. Nerem AT (2005) Bioengineered tissues: the science, the technology, and the industry. Orthod Craniofac Res 8:134–140
56. Andia DC, Cerri PS, Spolidorio LC (2006) Bone tissue: morphological and histophysiological aspects. J Dent 35:191–198
57. Herliansyah MK, Nasution DA, Shukor BA, Hamdi M, Ide-Ektessabi A, Wildan MW, Tontowi AE (2007). Preparation and characterization of natural hydroxyapatite: a comparative study of bovine bone hydroxyapatite and hydroxyapatite from calcite. In Mater Sci Forum 561: 1441–1444. Trans Tech Publications
58. Heidari F, Razavi M, Bahrololoom ME, Yazdimamaghani M, Tahriri M, Kotturi H, Tayebi L (2018) Evaluation of the mechanical properties, in vitro biodegradability and cytocompatibility of natural chitosan/hydroxyapatite/nano-Fe3O4 composite. Ceram Int 44(1):275–281
59. Obada DO, Dodoo-Arhin D, Dauda M, Anafi FO, Ahmed AS, Ajayi OA (2017) Physico-mechanical and gas permeability characteristics of kaolin based ceramic membranes prepared with a new pore-forming agent. Appl Clay Sci 150(2017):175–183
60. Sobczak A, Kida A, Kowalski Z, Wzorek Z (2009) Evaluation of the biomedical properties of hydroxyapatite obtained from bone waste. Pol J Chem Technol 11(1):37–43
61. Sobczak A, Kowalski Z, Wzorek Z (2009) Preparation of hydroxyapatite from animal bones. Acta Bioeng Biomech 11(4):23–28
62. Ozawa M, Suzuki S (2002) Microstructural development of natural hydroxyapatite originated from fish-bone waste through heat treatment. J Am Ceram Soc 85(5):1315–1317
63. Aghdam HA, Sanatizadeh E, Motififard M, Aghadavoudi F, Saber-Samandari S, Esmaeili S, Khandan A (2020) Effect of calcium silicate nanoparticle on surface feature of calcium phosphates hybrid bio-nanocomposite using for bone substitute application. Powder Technol 361:917–929
64. Gross KA, Saber-Samandari S (2009) Revealing mechanical properties of a suspension plasma sprayed coating with nanoindentation. Surf Coat Technol 203(20–21):2995–2999
65. Saber-Samandari S, Gross KA (2009) Nanoindentation reveals mechanical properties within thermally sprayed hydroxyapatite coatings. Surf Coat Technol 203(12):1660–1664
66. Saber-Samandari S, Gross KA (2009) Nanoindentation on the surface of thermally sprayed coatings. Surf Coat Technol 203(23):3516–3520
67. Layrolle P, Ito A, Tateishi T (1998) Sol-gel synthesis of amorphous calcium phosphate and sintering into microporous hydroxyapatite bioceramics. J Am Ceram Soc 81:1421–1428. https://doi.org/10.1111/j.1151-2916.1998.tb02499.x
68. Loo SCJ, Siew YE, Ho S, Boey FYC, Ma J (2008) Synthesis and hydrothermal treatment of nanostructured hydroxyapatite

of controllable sizes. J Mater Sci: Mater Med 19:1389–1397. https://doi.org/10.1007/s10856-007-3261-9
69. Pu'ad NM, Koshy P, Abdullah HZ, Idris MI, Lee TC (2019) Syntheses of hydroxyapatite from natural sources. Heliyon 5(5):e01588
70. Chaudhuri B, Mondal B, Modak DK, Pramanik K, Chaudhuri BK (2013) Preparation and characterization of nanocrystalline hydroxyapatite from egg shell and K2HPO4 solution. Mater Lett 97:148–150. https://doi.org/10.1016/j.matlet.2013.01.082
71. Ravaglioli A, Krajewski A (1992) Bioceramics: materials, properties, application. Chapman and Hall, London, pp 156–197
72. Ruksudjarit A, Pengpat K, Rujijanagul G, Tunkasiri T (2008) Synthesis and characterization of nanocrystalline hydroxyapatite from natural bovine bone. Curr Appl Phys 8(3–4):270–272
73. Ayatollahi MR, Yahya MY, Shirazi HA, Hassan SA (2015) Mechanical and tribological properties of hydroxyapatite nanoparticles extracted from natural bovine bone and the bone cement developed by nano-sized bovine hydroxyapatite filler. Ceram Int 41(9):10818–10827
74. Sun RX, Lv Y, Niu YR, Zhao XH, Cao DS, Tang J, Chen KZ (2017) Physicochemical and biological properties of bovine-derived porous hydroxyapatite/collagen composite and its hydroxyapatite powders. Ceram Int 43(18):16792–16798
75. Zhao F, Chen Z, Li R, Zhou J (2010) Ultra-sensitive detection of heavy metal ions in tap water by laser-induced breakdown spectroscopy with the assistance of electrical-deposition. Anal Methods 2(4):408–414
76. Akram M, Ahmed R, Shakir I, Ibrahim WAW, Hussain R (2014) Extracting hydroxyapatite and its precursors from natural resources. J Mater Sci 49(4):1461–1475
77. Haberko K, Bućko MM, Brzezińska-Miecznik J, Haberko M, Mozgawa W, Panz T, Zarębski J (2006) Natural hydroxyapatite: its behaviour during heat treatment. J Eur Ceram Soc 26(4–5):537–542
78. Janus AM, Faryna M, Haberko K, Rakowska A, Panz T (2008) Chemical and microstructural characterization of natural hydroxyapatite derived from pig bones. Microchim Acta 161(3–4):349–353
79. Panda NN, Pramanik K, Sukla LB (2014) Extraction and characterization of biocompatible hydroxyapatite from fresh water fish scales for tissue engineering scaffold. Bioprocess Biosyst Eng 37(3):433–440
80. Martin WA, Larson SL, Felt DR, Wright J, Griggs CS, Thompson M, Nestler CC (2008) The effect of organics on lead sorption onto Apatite II^{TM}. Appl Geochem 23(1):34–43
81. Sunil BR, Jagannatham M (2016) Producing hydroxyapatite from fish bones by heat treatment. Mater Lett 185:411–414
82. Paul S, Pal A, Choudhury AR, Bodhak S, Balla VK, Sinha A, Das M (2017) Effect of trace elements on the sintering effect of fish scale derived hydroxyapatite and its bioactivity. Ceram Int 43(17):15678–15684
83. Pon-On W, Suntornsaratoon P, Charoenphandhu N, Thongbunchoo J, Krishnamra N, Tang IM (2016) Hydroxyapatite from fish scale for potential use as bone scaffold or regenerative material. Mater Sci Eng, C 62:183–189
84. Kongsri S, Janpradit K, Buapa K, Techawongstien S, Chanthai S (2013) Nanocrystalline hydroxyapatite from fish scale waste: preparation, characterization and application for selenium adsorption in aqueous solution. Chem Eng J 215:522–532
85. Admassu W, Breese T (1999) Feasibility of using natural fishbone apatite as a substitute for hydroxyapatite in remediating aqueous heavy metals. J Hazard Mater 69(2):187–196
86. Ozawa M, Kanahara S (2005) Removal of aqueous lead by fish-bone waste hydroxyapatite powder. J Mater Sci 40(4):1037–1038
87. Wright J, Rice KR, Murphy B, Conca J (2004). PIMS using Apatite II™: How it works to remediate soil and water. In: RE Hinchee and B Alleman (Eds) Sustainable range management, Battelle Press, Columbus, OH www batelle org/bookstore, ISBN, 1–57477
88. Mondal B, Mondal S, Mondal A, Mandal N (2016) Fish scale derived hydroxyapatite scaffold for bone tissue engineering. Mater Charact 121:112–124
89. Venkatesan J, Qian ZJ, Ryu B, Thomas NV, Kim SK (2011) A comparative study of thermal calcination and an alkaline hydrolysis method in the isolation of hydroxyapatite from thunnus obesus bone. Biomed Mater 6(3):035003
90. Hosseinzadeh E, Davarpanah M, Nemati NH, Tavakoli SA (2014) Fabrication of a hard tissue replacement using natural hydroxyapatite derived from bovine bones by thermal decomposition method. Int J Organ Transplant Med 5(1):23
91. Londoño-Restrepo SM, Ramirez-Gutierrez CF, Del Real A, Rubio-Rosas E, Rodriguez-García ME (2016) Study of bovine hydroxyapatite obtained by calcination at low heating rates and cooled in furnace air. J Mater Sci 51(9):4431–4441
92. Saber-Samandari S, Alamara K, Saber-Samandari S, Gross KA (2013) Micro-Raman spectroscopy shows how the coating process affects the characteristics of hydroxylapatite. Acta Biomater 9(12):9538–9546
93. Saber-Samandari S, Alamara K, Saber-Samandari S (2014) Calcium phosphate coatings: morphology, micro-structure and mechanical properties. Ceram Int 40(1):563–572
94. Akamatsu N (1993) Artifacial bone and joints. Asian Med J 36:621–627
95. Hench L (1998) Bioceramics. J Am Ceram Soc 81:1705–2172
96. Bhuiyan D, Jablonsky M, Kolesov I, Middleton J, Wick T, Tannenbaum R (2015) Novel synthesis and characterization of a collagen-based biopolymer initiated by hydroxyapatite nanoparticles. Acta Biomater 15:181–190
97. Sharma C, Dinda AK, Potdar PD, Chou C-F, Mishra NC (2016) Fabrication and characterization of novel nano-biocomposite scaffold of chitosan–gelatin–alginate–hydroxyapatite for bone tissue engineering. Mater Sci Eng C 64:416–427
98. Socrates R, Sakthivel N, Rajaram A, Ramamoorthy U, Kalkura SN (2015) Novel fibrillar collagen–hydroxyapatite matrices loaded with silver nanoparticles for orthopedic application. Mater Lett 161:759–762
99. Chao SC, Wang M-J, Pai N-S, Yen S-K (2015) Preparation and characterization of gelatin–hydroxyapatite composite microspheres for hard tissue repair. Mater Sci Eng C 57:113–122
100. Morsy R, Ali SS, El-Shetehy M (2017) Development of hydroxyapatite-chitosan gel sunscreen combating clinical multidrug-resistant bacteria. J Mol Struct 1143:251–258
101. Al-Ahmady HH, Elazeem AAF, Ahmed NEMB, Shawkat WM, Elmasry M, Abdelrahman MA, Abderazik MA (2018) Combining autologous bone marrow mononuclear cells seeded on collagen sponge with nano hydroxyapatite, and platelet-rich fibrin: reporting a novel strategy for alveolar cleft bone regeneration. J Cranio-Maxillofac Surg 46(9):1593–1600
102. Fragal EH, Cellet TS, Fragal VH, Witt MA, Companhoni MV, UedaNakamura T, Silva R, Rubira AF (2018) Biomimetic nanocomposite based on hydroxyapatite mineralization over chemically modified cellulose nanowhiskers: an active platform for osteoblast proliferation. Int J Biol Macromol 125(2019):133–142
103. Murugan R, Ramakrishna S (2004) Nanostructured biomaterials. In: Nalwa HS (ed) Encyclopedia of nanoscience and nanotechnology, vol 7. American Scientific Publishers, California, pp 595–613
104. Shuai C, Yuan X, Yang W, Peng S, Qian G, Zhao Z (2021) Synthesis of a mace-like cellulose nanocrystal@ Ag nanosystem via in-situ growth for antibacterial activities of poly-L-lactide scaffold. Carbohydr Polym 262:117937

105. Boskey AL (2013) Natural and synthetic hydroxyapatites. Biomater Sci: Int Mater
106. Moerbeck FP, Barreto MA, Medrado ARAP, Amaral MTR, Moerbeck LG, Vale DS, Calasans-Maia MD (2019) Biological principles of nanostructured hydroxyapatite associated with metals: a literature review. Insights Biomed 4(3):13
107. Chen S, Shi Y, Zhang X, Ma J (2019) 3D printed hydroxyapatite composite scaffolds with enhanced mechanical properties. Ceram Int 45(8):10991–10996
108. Esmaeilkhanian A, Sharifianjazi F, Abouchenari A, Rouhani A, Parvin N, Irani M (2019) Synthesis and characterization of natural nano-hydroxyapatite derived from turkey femur-bone waste. Appl Biochem Biotechnol 189(3):919–932
109. Lü XY, Fan YB, Gu D, Cui W (2007). Preparation and characterization of natural hydroxyapatite from animal hard tissues. In Key engineering materials 342: pp. 213–216. Trans Tech Publications Ltd
110. Mezahi F, Oudadesse H, Harabi A, Lucas-Girot A, Le Gal Y, Chaair H, Cathelineau G (2009) Dissolution kinetic and structural behaviour of natural hydroxyapatite versus thermal treatment: comparison to synthetic hydroxyapatite. J Therm Anal Calorim 95(1):21–29
111. Barakat NA, Khil MS, Omran AM, Sheikh FA, Kim HY (2009) Extraction of pure natural hydroxyapatite from the bovine bones bio waste by three different methods. J Mater Process Technol 209(7):3408–3415
112. Ayed FB, Bouaziz J, Bouzouita K (2001) Calcination and sintering of fluorapatite under argon atmosphere. J Alloy Comp 322(1–2):238–245
113. Aarthy S, Thenmuhil D, Dharunya G, Manohar P (2019) Exploring the effect of sintering temperature on naturally derived hydroxyapatite for bio-medical applications. J Mater Sci: Mater Med 30(2):21
114. Foroughi MR, Karbasi S, Ebrahimi-Kahrizsangi R (2012) Physical and mechanical properties of a poly-3-hydroxybutyrate-coated nanocrystalline hydroxyapatite scaffold for bone tissue engineering. J Porous Mater 19(5):667–675
115. Chang C, Peng N, He M, Teramoto Y, Nishio Y, Zhang L (2013) Fabrication and properties of chitin/hydroxyapatite hybrid hydrogels as scaffold nano-materials. Carbohyd Polym 91(1):7–13
116. Baradaran S, Moghaddam E, Basirun WJ, Mehrali M, Sookhakian M, Hamdi M, Alias Y (2014) Mechanical properties and biomedical applications of a nanotube hydroxyapatite reduced graphene oxide composite. Carbon 69:32–45
117. Kim HL, Jung GY, Yoon JH, Han JS, Park YJ, Kim DG, Kim DJ (2015) Preparation and characterization of nano-sized hydroxyapatite/alginate/chitosan composite scaffolds for bone tissue engineering. Mater Sci Eng, C 54:20–25
118. Yazdanpanah Z, Bahrololoom ME, Hashemi B (2015) Evaluating morphology and mechanical properties of glass-reinforced natural hydroxyapatite composites. J Mech Behav Biomed Mater 41:36–42
119. Harabi E, Harabi A, Mezahi FZ, Zouai S, Karboua NE, Chehlatt S (2016) Effect of P2O5 on mechanical properties of porous natural hydroxyapatite derived from cortical bovine bones sintered at 1050 °C. Desalin Water Treat 57(12):5297–5302
120. Obada DO, Dauda ET, Abifarin JK, Bansod ND, Dodoo-Arhin D (2020) Mechanical measurements of pure and kaolin reinforced hydroxyapatite-derived scaffolds: a comparative study. Mater Today: Proc 38:2295–2300
121. Saber-Samandari S, Gross KA (2009) Micromechanical properties of single crystal hydroxyapatite by nanoindentation. Acta Biomater 5(6):2206–2212
122. Oliver WC, Pharr GM (2004) Measurement of hardness and elastic modulus by instrumented indentation: advances in understanding and refinements to methodology. J Mater Res 19:3–20
123. Saber-Samandari S, Gross KA (2011) Amorphous calcium phosphate offers improved crack resistance: a design feature from nature. Acta Biomater 7(12):4235–4241
124. Saber-Samandari S, Gross KA (2009) Micromechanical properties of single crystal hydroxyapatite by nanoindentation. Acta Biomater 5:2206–2212
125. Joneidi Yekta H, Shahali M, Khorshidi S, Rezaei S, Montazeran AH, Samandari SS, Khandan A (2018) Mathematically and experimentally defined porous bone scaffold produced for bone substitute application. Nanomed J 5(4):227–234
126. Yang W, Zhong Y, He C, Peng S, Yang Y, Qi F, Shuai C (2020) Electrostatic self-assembly of pFe3O4 nanoparticles on graphene oxide: a co-dispersed nanosystem reinforces PLLA scaffolds. J Adv Res 24:191–203
127. Yaszemski MJ, Trantolo DJ, Lewandrowski KU, Hasirci V, Altobelli DE, Wise DL (2004) Biomaterials in orthopedics, 2nd edn. Marcel Dekker Inc., New York
128. Obada DO, Salami KA, Oyedeji AN, Fasanya OO, Suleiman MU, Ibisola BA, Dauda ET (2021) Solution combustion synthesis of strontium-doped hydroxyapatite: effect of sintering and low compaction pressure on the mechanical properties and physiological stability. Mater Lett 304:130613
129. Gilmore RS, Katz JL (1982) Elastic properties of apatites. J Mater Sci 17(4):1131–1141
130. LeGeros RZ, LeGeros JP (1993) Dense hydroxyapatite, In: An Introduction to bioceramics, pp. 139–180
131. Martin RI, Brown PW (1995) Mechanical properties of hydroxyapatite formed at physiological temperature. J Mater Sci Mater Med 6(3):138–143
132. Sabree I, Gough JE, Derby B (2015) Mechanical properties of porous ceramic scaffolds: influence of internal dimensions. Ceram Int 41(7):8425–8432
133. Karageorgiou V, Kaplan D (2005) Porosity of 3D biomaterial scaffolds and osteogenesis. Biomaterials 26(27):5474–5491
134. Murugan R, Ramakrishna S (2005) Development of nanocomposites for bone grafting. Compos Sci Technol 65(15–16):2385–2406
135. Landi E, Tampieri A, Celotti G, Sprio S (2000) Densification behaviour and mechanisms of synthetic hydroxyapatites. J Eur Ceram Soc 20(14–15):2377–2387
136. Munar ML, Udoh KI, Ishikawa K, Matsuya S, Nakagawa M (2006) Effects of sintering temperature over 1300 °C on the physical and compositional properties of porous hydroxyapatite foam. Dent Mater J 25(1):51–58
137. Yang L, Sheldon BW, Webster TJ (2010) Nanophase ceramics for improved drug delivery. Am Ceram Soc Bull 89(2):24–32
138. Ioku K, Yamauchi S, Fujimori H, Goto S, Yoshimura M (2002) Hydrothermal preparation of fibrous apatite and apatite sheet. Solid State Ionics 151(1–4):147–150
139. Kizuki T, Ohgaki M, Katsura M, Nakamura S, Hashimoto K, Toda Y, Yamashita K (2003) Effect of bone-like layer growth from culture medium on adherence of osteoblast-like cells. Biomaterials 24(6):941–947
140. Gibson P, Schreuder-Gibson H, Rivin D (2001) Transport properties of porous membranes based on electrospun nanofibers. Colloids Surf, A 187:469–481
141. Rhee SH, Tanaka J (2001) Synthesis of a hydroxyapatite/collagen/chondroitin sulfate nanocomposite by a novel precipitation method. J Am Ceram Soc 84(2):459–461
142. Rhee SH, Suetsugu Y, Tanaka J (2001) Biomimetic configurational arrays of hydroxyapatite nanocrystals on bio-organics. Biomaterials 22(21):2843–2847

143. Tenhuisen KS, Martin RI, Klimkiewicz M, Brown PW (1995) Formation and properties of a synthetic bone composite: hydroxyapatite–collagen. J Biomed Mater Res 29(7):803–810
144. Zhang S, Gonsalves KE (1997) Preparation and characterization of thermally stable nanohydroxyapatite. J Mater Sci: Mater Med 8(1):25–28
145. Ramakrishna S, Mayer J, Wintermantel E, Leong KW (2001) Biomedical applications of polymer-composite materials: a review. Compos Sci Technol 61(9):1189–1224